Mechanical Systems and Signal Processing 60-61 (2015) 583–603

Contents lists available at ScienceDirect

Mechanical Systems and Signal Processing

journal homepage: www.elsevier.com/locate/ymssp

Nonlocal normal modes in nanoscale dynamical systems

S. Adhikari [a,*], D. Gilchrist [a], T. Murmu [b], M.A. McCarthy [c]

[a] College of Engineering, Swansea University, Swansea SA2 8PP, UK
[b] School of Engineering, University of the West of Scotland, Paisley, PA1 2BE, UK
[c] Department of Mechanical, Aeronautical and Biomedical Engineering, Irish Centre for Composites Research, Materials and Surface Science Institute, University of Limerick, Limerick, Ireland

ARTICLE INFO

Article history:
Received 26 May 2014
Received in revised form
6 November 2014
Accepted 9 December 2014
Available online 29 January 2015

Keywords:
Normal modes
Nonlocal mechanics
Finite element
Nonlocal frequency

ABSTRACT

This paper introduces the idea of nonlocal normal modes arising in the dynamic analysis of nanoscale structures. A nonlocal finite element approach is developed for the axial vibration of nanorods, bending vibration of nanobeams and transverse vibration of nanoplates. Explicit expressions of the element mass and stiffness matrices are derived in closed-form as functions of a length-scale parameter. In general the mass matrix can be expressed as a sum of the classical local mass matrix and a nonlocal part. The nonlocal part of the mass matrix is scale-dependent and vanishes for systems with larger lengths. Classical modal analysis and perturbation method are used to understand the dynamic behaviour of discrete nonlocal systems in the light of classical local systems. The conditions for the existence of classical normal modes for undamped and damped nonlocal systems are established. Closed-form approximate expressions of nonlocal natural frequencies, modes and frequency response functions are derived. Results derived in the paper are illustrated using examples of axial and bending vibration of nanotubes and transverse vibration of graphene sheets.

1. Introduction

Nanoscale systems, such as those fabricated from simple and complex nanorods, nanobeams [1] and nanoplates, have attracted keen interest among scientists and engineers. Examples of one-dimensional nanoscale objects include (nanorod and nanobeam) carbon nanotubes [2], zinc oxide (ZnO) nanowires and boron nitride (BN) nanotubes, while two-dimensional nanoscale objects include graphene sheets [3] and BN nanosheets [4]. These nanoscale entities or nanostructures are found to have exciting mechanical, chemical, electrical, optical and electronic properties. Nanostructures are being used in the field of nanoelectronics, nanodevices, nanosensors, nanooscillators, nanoactuators, nanobearings, and micromechanical resonators, transporter of drugs, hydrogen storage, electrical batteries, solar cells, nanocomposites and nanooptomechanical systems (NOMS). Understanding the dynamics of nanostructures is crucial for the development of future generation applications in these areas.

Experiments at the nanoscale can be difficult as many parameters need to be taken care of. On the other hand, atomistic computation methods such as molecular dynamic (MD) simulations [5] are computationally prohibitive for nanostructures with large numbers of atoms. Thus continuum mechanics is an important tool for modelling, understanding and predicting

* Corresponding author. Tel.: +44 1792 602088.
E-mail address: S.Adhikari@swansea.ac.uk (S. Adhikari).

http://dx.doi.org/10.1016/j.ymssp.2014.12.004
0888-3270/

physical behaviour of nanostructures. Although continuum models based on classical elasticity are able to predict the general behaviour of nanostructures, they lack the accountability of effects arising from the small-scale. At small-scale the theory and laws of classical elasticity may not hold. Consequently for accurate predictions, the employability of the classical continuum models have been questioned in the analysis of nanostructures and nanoscale systems. To address this, size-dependent continuum based methods [6–9] are getting in popularity in the modelling of small sized structures as they offer much faster solutions than molecular dynamic simulations for various nanoengineering problems. Currently research efforts are undergoing to bring in the size-effects within the formulation by modifying the traditional classical mechanics. One popularly used size-dependant theory is the nonlocal elasticity theory pioneered by Eringen [10], and applied to nanotechnology by Peddieson et al. [11]. The theory of nonlocal elasticity (nonlocal continuum mechanics) is being increasingly used for efficient analysis of nanostructures viz. nanorods [12,13], nanobeams [14], nanoplates [15,16], nanorings [17], carbon nanotubes [18,19], graphenes [20,21], nanoswitches [22] and microtubules [23]. Nonlocal elasticity accounts for the small-scale effects at the atomistic level. At nanometer scales, size effects often become prominent. Both experimental and atomistic simulation results have shown a significant size-effect in the mechanical properties when the dimensions of these structures become small [24,25]. In the nonlocal elasticity theory the small-scale effects are captured by assuming that the stress at a point as a function of the strains at all points in the domain. Nonlocal theory considers long-range inter-atomic interaction and yields results dependent on the size of a body [10]. Some of the drawbacks of the classical continuum theory could be efficiently avoided and size-dependent phenomena can be explained by the nonlocal elasticity theory. A good review on nonlocal elasticity and application to nanostructures can be found in Ref [26].

Several researchers have used nonlocal theory for dynamic analysis of continuum systems such as nanorods, nanobeams and nanoplates. Nanorods have found application in energy harvesting, light emitting devices and microelectromechanical systems (MEMS). Using nonlocal elasticity, various work on mechanical behaviour of nanorods [12,13,27–29] were reported. Numerous works are seen in the literature regarding analysis (mainly structural) of nanobeams using nonlocal elasticity [26] and coupled nanobeams [14]. The work on nanobeams is related to carbon nanotubes, boron nitride nanotubes and ZnO nanowires. Nanoplate models have been used to represent two-dimensional nanostructures such as graphene sheets and BN sheets. Several works on dynamics of nanoplates using nonlocal theory are available in literature [30,31].

From the brief literature review it is clear that significant research efforts have taken place in the analysis of nanostructures modelled as a continuum. While the results have given significant insights, the analysis is normally restricted to single-structure (e.g, a beam or a plate) with simple boundary conditions and no damping. In the future complex nanoscale structures will be used for next generation nanoelectro-mechanical systems. Therefore, it is necessary to have the ability for design and analysis of damped built-up structures. The finite element approach for nanoscale structures can provide this generality. Work on nonlocal finite elements is in its infancy stage. Pisano et al. [32] reported a finite element procedure for nonlocal integral elasticity. Chang [33] studied the small scale effects on axial vibration of non-uniform and nonhomogeneous nanorods by using the theory of nonlocal elasticity and the finite element method. Narendar and Gopalakrishnan [34] used the concept of nonlocal elasticity and applied it for the development of a spectral finite element (SFE) for analysis of nanorods. Recently Adhikari et al. [35] reported the free and forced axial vibrations of damped nonlocal rods using dynamic nonlocal finite element analysis. Similar to the few works on nonlocal finite element analysis of nanorods, not many works were reported on the nonlocal finite element formulation of nanobeams (carbon nanotubes). Phadikar and Pradhan [30] have proposed basic finite element formulations for a nonlocal elastic EulerBernoulli beam using the Galerkin technique. Studies were carried out for bending, free vibration and buckling for nonlocal beam with four classical boundary conditions. Pradhan [36] updated the work of nonlocal finite element to Timoshenko beam theory and applied it to carbon nanotubes. With the finite element analysis bending, buckling and vibration for nonlocal beams with clamped–clamped, hinged–hinged, clamped–hinged and clamped-free boundary conditions were illustrated. The basic nonlocal finite elements of undamped two-dimensional nanoplates (such as graphene sheets) were reported by Phadikar and Pradhan [30]. Recently, Ansari et al. [37] developed nonlocal finite element model for vibration of embedded multi-layered graphene sheets. The proposed finite elements were based on the Mindlin-type equations of motion coupled together through the van der Waals interaction. Vibrational characteristics of multi-layered graphene sheets with different boundary conditions embedded in an elastic medium were considered.

The majority of the reported works on nonlocal finite element analysis consider free vibration studies where the effect of non-locality on the undamped eigensolutions has been studied. Damped nonlocal systems and forced vibration response analysis have received little attention. On the other hand, significant body of literature is available [38–40] on finite element analysis of local dynamical systems. It is necessary to extend the ideas of local modal analysis to nonlocal systems to gain qualitative as well as quantitative understanding. This way, the dynamic behaviour of general nonlocal discretised systems can be explained in the light of well known established theories of discrete local systems. The purpose of this paper is to make contributions in this open area.

The paper is organised as follows. In Section 2 we introduce the nonlocal finite element formulation for the axial vibration of rods, bending vibration of beams and transverse vibration of plates. Explicit expressions of element mass and stiffness matrices for the three systems are derived. Modal analysis of discrete nonlocal dynamical systems is discussed in Section 3. The conditions for the existence of classical normal modes, approximations for nonlocal frequencies and modes are proposed. In Section 4, dynamic response of damped nonlocal systems and approximation to the frequency response function are discussed. Analytical results, including the approximations of the nonlocal natural frequencies and modes, are numerically illustrated for the three systems in Section 5. In Section 6 some conclusions are drawn based on the theoretical and numerical results obtained in the paper.

2. Finite element modelling of nonlocal dynamic systems

2.1. Brief overview of nonlocal elasticity

In this section and the next three subsections, we review the fundamental principle of nonlocal elasticity theory and give the equations of motion for axial vibration of nanorods, bending vibration of nanobeams and flexural vibration of thin nanoplates. Equations of motions are not derived here, but relevant references are given for background. According to Eringen [10], the basic equations for nonlocal anisotropic linear homogenous nonlocal elastic body neglecting the body force can be expressed as

$$\begin{aligned}&\sigma_{ij,j}=0,\\&\sigma_{ij}(\mathbf{x})=\int_V \phi(|\mathbf{x}-\mathbf{x}'|,\alpha)\mathbf{t}_{ij}d\mathbf{V}(\mathbf{x}'),\quad \forall x\in\mathbf{V}\\&\mathbf{t}_{ij}=H_{ijkl}\epsilon_{kl},\\&\epsilon_{ij}=1/2(u_{i,j}+u_{j,i}\end{aligned}\tag{1}$$

The terms σ_{ij}, t_{ij}, ϵ_{kl} and H_{ijkl} are the nonlocal stress, classical stress, classical strain and fourth order elasticity tensors respectively. The volume integral is over the region $\mathbf{V}$ occupied by the body. Eq. (1) couples the stress due to nonlocal elasticity and the stress due to classical elasticity. The kernel function $\phi(|\mathbf{x}-\mathbf{x}'|,\alpha)$ is the nonlocal modulus. The nonlocal modulus acts as an attenuation function incorporating into constitutive equations the nonlocal effects at the reference point $\mathbf{x}$ produced by local strain at the source $\mathbf{x}'$. The term $|\mathbf{x}-\mathbf{x}'|$ represents the distance in the Euclidean form and α is a material constant that depends on the internal (e.g. lattice parameter, granular size, distance between the C–C bonds) and external characteristics lengths (e.g. crack length and wave length). Material constant α is defined as $\alpha=(e_0a)l$. Here e_0 is a constant for calibrating the model with experimental results and other validated models. The parameter e_0 is estimated such that the relations of the nonlocal elasticity model could provide satisfactory approximation to the atomic dispersion curves of the plane waves with those obtained from the atomistic lattice dynamics. The terms a and l are the internal (e.g. lattice parameter, granular size, and distance between C–C bonds) and external characteristics lengths (e.g. crack length and wave length) of the nanostructure. Eq. (1) effectively shows that in nonlocal theory, the stress at a point is a function of the strains at all points in the domain. The classical elasticity can be viewed as a special cade when the kernel function becomes a Dirac delta function.

The direct use of Eq. (1) in boundary value problems results in integro-partial differential equations and they are generally difficult to solve analytically. For this reason, a differential form of nonlocal elasticity equation is often beneficial. According to Eringen [10], this can be achieved for a special case of the kernel function given by

$$\phi(|x-x'|,\alpha)=(2\pi\ell^2\alpha^2)K_0(\sqrt{x\bullet x}/\ell\alpha)\tag{2}$$

Here K_0 is the modified Bessel function. The equation of motion in terms of nonlocal elasticity can be expressed as

$$\sigma_{ij,j}+f_i=\rho\ddot{u}_i\tag{3}$$

where f_i, ρ and u_i are the components of the body forces, mass density, and the displacement vector, respectively. The terms i,j takes up the symbols x,y, and z. The operator $(\ddot{\bullet})$ denotes double derivative with respect to time. Assuming the kernel function ϕ as the Greens function, Eringen [10] proposed a differential form of the nonlocal constitutive relation as

$$\sigma_{ij,j}+\mathcal{L}(f_i-\rho\ddot{u}_i)=0\tag{4}$$

where

$$\mathcal{L}(\bullet)=[1-(e_0a)^2\nabla^2](\bullet)\tag{5}$$

and ∇^2 is the Laplacian. Using this equation the nonlocal constitutive stress–strain relation can be simplified as

$$(1-\alpha^2\, l^2\nabla^2)\sigma_{ij}=t_{ij}\tag{6}$$

One can use this relationship and derive the equation of motion using conventional variational principle. In the next subsections we consider the dynamics of nonlocal road, beam and plate using this approach.

2.2. Axial vibration of nanorods

The equation of motion of axial vibration for a damped nonlocal rod can be expressed as [41,12,42,35]

$$EA\frac{\partial^2U(x,t)}{\partial x^2}+\widehat{c}_1\frac{\partial^3U(x,t)}{\partial x^2\partial t}=\widehat{c}_2\frac{\partial U(x,t)}{\partial t}+\left(1-(e_0a)^2\frac{\partial^2}{\partial x^2}\right)\left\{m\frac{\partial^2U(x,t)}{\partial t^2}+F(x,t)\right\}\tag{7}$$

In the above equation EA is the axial rigidity, m is mass per unit length, e_0a is the nonlocal parameter [10], $U(x,t)$ is the axial displacement, $F(x,t)$ is the applied force, x is the spatial variable, and t is the time. The constant $\widehat{c}_1$ is the strain-rate-dependent viscous damping coefficient and $\widehat{c}_2$ is the velocity-dependent viscous damping coefficient. We consider an element of length ℓ_e with axial stiffness EA and mass per unit length m. An element of the axially vibrating rod is shown

in Fig. 1. This element has two degrees of freedom and there are two shape functions $N_1(x)$ and $N_2(x)$. The shape function matrix for the axial deformation [40] can be given by

$$\mathbf{N}(x) = [N_1(x), N_2(x)]^T = [1 - x/\ell_e, x/\ell_e]^T \tag{8}$$

Using this the stiffness matrix can be obtained using the conventional variational formulation as

$$\mathbf{K}_e = EA \int_0^{\ell_e} \frac{d\mathbf{N}(x)}{dx} \frac{d\mathbf{N}^T(x)}{dx}\, dx = \frac{EA}{\ell_e} \begin{bmatrix} 1 & -1 \\ -1 & 1 \end{bmatrix} \tag{9}$$

The mass matrix for the nonlocal element can be obtained as

$$\begin{aligned} \mathbf{M}_e &= m \int_0^{\ell_e} \mathbf{N}(x)\mathbf{N}^T(x)\, dx + m(e_0 a)^2 \int_0^{\ell_e} \frac{d\mathbf{N}(x)}{dx} \frac{d\mathbf{N}^T(x)}{dx}\, dx \\ &= \frac{m\ell_e}{6} \begin{bmatrix} 2 & 1 \\ 1 & 2 \end{bmatrix} + \left(\frac{e_0 a}{\ell_e}\right)^2 m\ell_e \begin{bmatrix} 1 & -1 \\ -1 & 1 \end{bmatrix} \end{aligned} \tag{10}$$

For the special case when the rod is local, the mass matrix derived above reduces to the classical mass matrix [40,43] as $e_0 a = 0$. Therefore for a nonlocal rod, the element stiffness matrix is identical to that of a classical local rod but the element mass has an additive term which is dependent on the nonlocal parameter.

2.3. Bending vibration of nanobeams

For the bending vibration of a nonlocal damped beam, the equation of motion can be expressed by [36,41,44]

$$EI \frac{\partial^4 V(x,t)}{\partial x^4} + m\left(1 - (e_0 a)^2 \frac{\partial^2}{\partial x^2}\right)\left\{\frac{\partial^2 V(x,t)}{\partial t^2}\right\} + \widehat{c}_1 \frac{\partial^5 V(x,t)}{\partial x^4 \partial t} + \widehat{c}_2 \frac{\partial V(x,t)}{\partial t} = \left(1 - (e_0 a)^2 \frac{\partial^2}{\partial x^2}\right)\{F(x,t)\} \tag{11}$$

In the above equation EI is the bending rigidity, m is mass per unit length, $e_0 a$ is the nonlocal parameter, $V(x,t)$ is the transverse displacement and $F(x,t)$ is the applied force. The constant $\widehat{c}_1$ is the strain-rate-dependent viscous damping coefficient and $\widehat{c}_2$ is the velocity-dependent viscous damping coefficient. We consider an element of length ℓ_e with bending stiffness EI and mass per unit length m. An element of the beam is shown in Fig. 2. This element has four degrees of freedom and there are four shape functions. The shape function matrix for the bending deformation [40] can be given by

$$\mathbf{N}(x) = [N_1(x), N_2(x), N_3(x), N_4(x)]^T \tag{12}$$

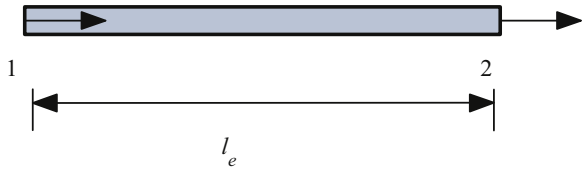

Fig. 1. A nonlocal element for the axially vibrating rod with two nodes. It has two degrees of freedom and the displacement field within the element is expressed by linear shape functions.

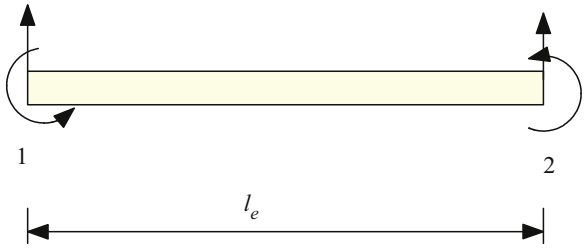

Fig. 2. A nonlocal element for the bending vibration of a beam. It has two nodes and four degrees of freedom. The displacement field within the element is expressed by cubic shape functions.

where

$$N_1(x)=1-3\frac{x^2}{\ell_e^2}+2\frac{x^3}{\ell_e^3},\quad N_2(x)=x-2\frac{x^2}{\ell_e}+\frac{x^3}{\ell_e^2},$$
$$N_3(x)=3\frac{x^2}{\ell_e^2}-2\frac{x^3}{\ell_e^3},\qquad N_4(x)=-\frac{x^2}{\ell_e}+\frac{x^3}{\ell_e^2} \tag{13}$$

Using this, the stiffness matrix can be obtained using the conventional variational formulation [43] as

$$\mathbf{K}_e=EI\int_0^{\ell_e}\frac{d^2\mathbf{N}(x)}{dx^2}\frac{d^2\mathbf{N}^T(x)}{dx^2}\,dx=\frac{EI}{\ell_e^3}\begin{bmatrix}12 & 6\ell_e & -12 & 6\ell_e\\ 6\ell_e & 4\ell_e^2 & -6\ell_e & 2\ell_e^2\\ -12 & -6\ell_e & 12 & -6\ell_e^2\\ 6\ell_e & 2\ell_e^2 & -6\ell_e & 4\ell_e^2\end{bmatrix} \tag{14}$$

The mass matrix for the nonlocal element can be obtained as

$$\mathbf{M}_e=m\int_0^{\ell_e}\mathbf{N}(x)\mathbf{N}^T(x)\,dx+m(e_0a)^2\int_0^{\ell_e}\frac{d\mathbf{N}(x)}{dx}\frac{d\mathbf{N}^T(x)}{dx}\,dx$$
$$=\frac{m\ell_e}{420}\begin{bmatrix}156 & 22\ell_e & 54 & -13\ell_e\\ 22\ell_e & 4\ell_e^2 & 13\ell_e & -3\ell_e^2\\ 54 & 13\ell_e & 156 & -22\ell_e\\ -13\ell_e & -3\ell_e^2 & -22\ell_e & 4\ell_e^2\end{bmatrix}+\left(\frac{e_0a}{\ell_e}\right)^2\frac{m\ell_e}{30}\begin{bmatrix}36 & 3\ell_e & -36 & 3\ell_e\\ 3\ell_e & 4\ell_e^2 & -3\ell_e & -\ell_e^2\\ -36 & -3\ell_e & 36 & -3\ell_e\\ 3\ell_e & -\ell_e^2 & -3\ell_e & 4\ell_e^2\end{bmatrix} \tag{15}$$

For the special case when the beam is local, the mass matrix derived above reduces to the classical mass matrix [40,43] as $e_0a=0$.

2.4. Transverse vibration of nanoplates

For the transverse bending vibration of a nonlocal damped thin plate, the equation of motion can be expressed by [15]

$$D\nabla^4V(x,y,t)+m\left(1-(e_0a)^2\nabla^2\right)\left\{\frac{\partial^2V(x,y,t)}{\partial t^2}\right\}+\widehat{c}_1\nabla^4\frac{\partial V(x,y,t)}{\partial x^4\partial t}+\widehat{c}_2\frac{\partial V(x,y,t)}{\partial t}=\left(1-(e_0a)^2\nabla^2\right)\{F(x,y,t)\} \tag{16}$$

In the above equation $\nabla^2=(\partial^2/\partial x^2+\partial^2/\partial x^2)$ is the differential operator, $D=Eh^3/12(1-\nu^2)$ is the bending rigidity, h is the thickness, ν is the Poisson's ratio, m is mass per unit area, e_0a is the nonlocal parameter, $V(x,y,t)$ is the transverse displacement and $F(x,y,t)$ is the applied force. The constant $\widehat{c}_1$ is the strain-rate-dependent viscous damping coefficient and $\widehat{c}_2$ is the velocity-dependent viscous damping coefficient. We consider an element of dimension $2c\times 2b$ with bending stiffness D and mass per unit area m. An element of the plate is shown in Fig. 3 together with the local coordinate system. The shape function matrix for the bending deformation is a 12×1 vector [43] and can be expressed as

$$\mathbf{N}(x,y)=\mathbf{C}_e^{-1}\boldsymbol{\alpha}(x,y) \tag{17}$$

Here the vector of polynomials is given by

$$\boldsymbol{\alpha}(x,y)=[1\ x\ y\ x^2\ xy\ y^2\ x^3\ x^2y\ xy^2\ y^3\ x^3y\ xy^3]^T \tag{18}$$

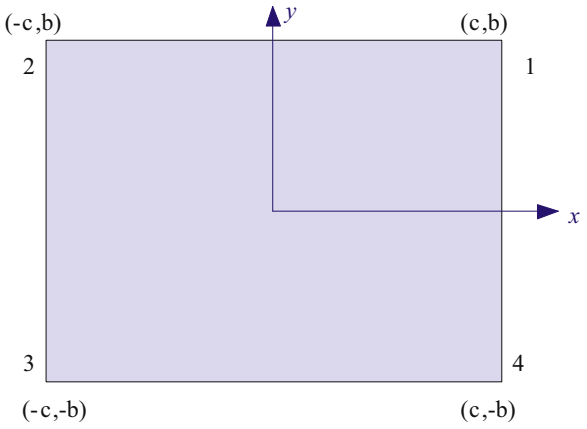

Fig. 3. A nonlocal element for the bending vibration of a plate. It has four nodes and twelve degrees of freedom. The displacement field within the element is expressed by cubic shape functions in both directions.

and the coefficient matrix can be obtained as

$$\mathbf{C}_e^{-1} = \frac{1}{8a^3b^3} \times \begin{bmatrix} 2c^3b^3 & c^3b^4 & c^4b^3 & 2c^3b^3 & c^3b^4 & -b^3c^4 & 2c^3b^3 & -c^3b^4 & -c^4b^3 & 2c^3b^3 & -c^3b^4 & c^4b^3 \\ -3c^2b^3 & -c^2b^4 & -c^3b^3 & 3c^2b^3 & c^2b^4 & -c^3b^3 & 3c^2b^3 & -c^2b^4 & -c^3b^3 & -3c^2b^3 & c^2b^4 & -c^3b^3 \\ -3c^3b^2 & -c^3b^3 & -c^4b^2 & -3c^3b^2 & -c^3b^3 & c^4b^2 & 3c^3b^2 & -c^3b^3 & -c^4b^2 & 3c^3b^2 & -c^3b^3 & c^4b^2 \\ 0 & 0 & -c^2b^3 & 0 & 0 & c^2b^3 & 0 & 0 & c^2b^3 & 0 & 0 & -c^2b^3 \\ 4c^2b^2 & c^2b^3 & c^3b^2 & -4c^2b^2 & -c^2b^3 & c^3b^2 & 4c^2b^2 & -c^2b^3 & -c^3b^2 & -4c^2b^2 & c^2b^3 & -c^3b^2 \\ 0 & -c^3b^2 & 0 & 0 & -c^3b^2 & 0 & 0 & c^3b^2 & 0 & 0 & c^3b^2 & 0 \\ b^3 & 0 & cb^3 & -b^3 & 0 & cb^3 & -b^3 & 0 & cb^3 & b^3 & 0 & cb^3 \\ 0 & 0 & c^2b^2 & 0 & 0 & -c^2b^2 & 0 & 0 & c^2b^2 & 0 & 0 & -c^2b^2 \\ 0 & c^2b^2 & 0 & 0 & -c^2b^2 & 0 & 0 & c^2b^2 & 0 & 0 & -c^2b^2 & 0 \\ c^3 & c^3b & 0 & c^3 & c^3b & 0 & -c^3 & c^3b & 0 & -c^3 & c^3b & 0 \\ -b^2 & 0 & -cb^2 & b^2 & 0 & -cb^2 & -b^2 & 0 & cb^2 & b^2 & 0 & cb^2 \\ -c^2 & -c^2b & 0 & c^2 & c^2b & 0 & -c^2 & c^2b & 0 & c^2 & -c^2b & 0 \end{bmatrix} \tag{19}$$

Using the shape functions in Eq. (17), the stiffness matrix can be obtained using the conventional variational formulation [43] as

$$\mathbf{K}_e = \int_{A_e} \mathbf{B}^T \mathbf{E} \mathbf{B}\, dA_e \tag{20}$$

In the preceding equation **B** is the strain-displacement matrix, and the matrix **E** is given by

$$\mathbf{E} = D \begin{bmatrix} 1 & \nu & 0 \\ \nu & 1 & 0 \\ 0 & 0 & \frac{1-\nu}{2} \end{bmatrix} \tag{21}$$

Evaluating the integral in Eq. (20), we can obtain the element stiffness matrix in closed-form as

$$\mathbf{K}_e = \frac{Eh^3}{12(1-\nu^2)} \mathbf{C}^{-1^T} \mathbf{k}_e \mathbf{C}^{-1} \tag{22}$$

where

$$\mathbf{k}_e = \begin{bmatrix} 0 & & & & & & & & & & & \\ 0 & 0 & & & & & & & & & & \\ 0 & 0 & 0 & & & & & & & & & \\ 0 & 0 & 0 & k_{e_{44}} & & & & & & & & \\ 0 & 0 & 0 & 0 & k_{e_{55}} & & & & & & & \\ 0 & 0 & 0 & k_{e_{64}} & 0 & k_{e_{66}} & & & & & & \\ 0 & 0 & 0 & 0 & 0 & 0 & k_{e_{77}} & & & & & \\ 0 & 0 & 0 & 0 & 0 & 0 & 0 & k_{e_{88}} & & & & \\ 0 & 0 & 0 & 0 & 0 & 0 & k_{e_{97}} & 0 & k_{e_{99}} & & & \\ 0 & 0 & 0 & 0 & 0 & 0 & 0 & k_{e_{108}} & 0 & k_{e_{1010}} & & \\ 0 & 0 & 0 & 0 & k_{e_{115}} & 0 & 0 & 0 & 0 & 0 & k_{e_{1111}} & \\ 0 & 0 & 0 & 0 & k_{e_{125}} & 0 & 0 & 0 & 0 & 0 & k_{e_{1211}} & k_{e_{1212}} \end{bmatrix} \tag{23}$$

with

$$k_{e_{44}} = 16cb, \quad k_{e_{55}} = 8cb(1-\nu), \quad k_{e_{64}} = 16\nu cb$$

$$k_{e_{66}} = 16cb, \quad k_{e_{77}} = 48c^3b, \quad k_{e_{88}} = \frac{16cb((2-2\nu)c^2+b^2)}{3}$$

$$k_{e_{97}} = 16\nu c^3 b, \quad k_{e_{99}} = \frac{16cb(c^2+2(1-\nu)b^2)}{3}, \quad k_{e_{10\,8}} = 16\nu cb^2$$

$$k_{e_{10\,10}} = 48cb^3, \quad k_{e_{11\,5}} = 8(1-\nu)c^3 b, \quad k_{e_{11\,11}} = 4c^3 b\left(\frac{9(1-\nu)c^2}{5} + 4b^2\right)$$

$$k_{e_{12\,5}} = 8(1-\nu)cb^3, \quad k_{e_{12\,11}} = 8(\nu+1)c^3 b^3, \quad k_{e_{12\,12}} = \frac{8\,cb^3(10c^2+9(1-\nu)b^2)}{5}$$

The mass matrix for the nonlocal element can be obtained as

$$\mathbf{M}_e = \rho h \int_{A_e} \left\{ \mathbf{N}(x,y)\mathbf{N}^T(x,y) + (e_0 a)^2 \left(\frac{\partial \mathbf{N}(x,y)}{\partial x}\frac{d\mathbf{N}^T(x,y)}{dx} + \frac{\partial \mathbf{N}(x,y)}{\partial x}\frac{d\mathbf{N}^T(x,y)}{dx} \right) \right\} dA_e$$

$$= \mathbf{M}_{0_e} + \left(\frac{e_0 a}{c}\right)^2 \mathbf{M}_{x_e} + \left(\frac{e_0 a}{b}\right)^2 \mathbf{M}_{y_e} \tag{24}$$

The three matrices appearing in the above expression can be obtained in closed-form as

$$\mathbf{M}_{0_e} = \frac{\rho hcb}{3150} \times \begin{bmatrix} 1727 & 461b & 461c & 613 & 199b & -274c & 197 & -116b & -116c & 613 & -274b & 199c \\ 461b & 160b^2 & 126cb & 199b & 80b^2 & -84cb & 116b & -60b^2 & -56cb & 274b & -120b^2 & 84cb \\ 461c & 126cb & 160c^2 & 274c & 84cb & -120c^2 & 116c & -56cb & -60c^2 & 199c & -84cb & 80c^2 \\ 613 & 199b & 274c & 1727 & 461b & -461c & 613 & -274b & -199c & 197 & -116b & 116c \\ 199b & 80b^2 & 84cb & 461b & 160b^2 & -126cb & 274b & -120b^2 & -84cb & 116b & -60b^2 & 56cb \\ -274c & -84cb & -120c^2 & -461c & -126cb & 160c^2 & -199c & 84cb & 80c^2 & -116c & 56cb & -60c^2 \\ 197 & 116b & 116c & 613 & 274b & -199c & 1727 & -461b & -461c & 613 & -199b & 274c \\ -116b & -60b^2 & -56cb & -274b & -120b^2 & 84cb & -461b & 160b^2 & 126cb & -199b & 80b^2 & -84cb \\ -116c & -56cb & -60c^2 & -199c & -84cb & 80c^2 & -461c & 126cb & 160c^2 & -274c & 84cb & -120c^2 \\ 613 & 274b & 199c & 197 & 116b & -116c & 613 & -199b & -274c & 1727 & -461b & 461c \\ -274b & -120b^2 & -84cb & -116b & -60b^2 & 56cb & -199b & 80b^2 & 84cb & -461b & 160b^2 & -126cb \\ 199c & 84cb & 80c^2 & 116c & 56cb & -60c^2 & 274c & -84cb & -120c^2 & 461c & -126cb & 160c^2 \end{bmatrix} \tag{25}$$

$$\mathbf{M}_{x_e} = \frac{\rho hcb}{630} \times \begin{bmatrix} 276 & 66b & 42c & -276 & -66b & 42c & -102 & 39b & 21c & 102 & -39b & 21c \\ 66b & 24b^2 & 0 & -66b & -24b^2 & 0 & -39b & 18b^2 & 0 & 39b & -18b^2 & 0 \\ 42c & 0 & 112c^2 & -42c & 0 & -28c^2 & -21c & 0 & -14c^2 & 21c & 0 & 56c^2 \\ -276 & -66b & -42c & 276 & 66b & -42c & 102 & -39b & -21c & -102 & 39b & -21c \\ -66b & -24b^2 & 0 & 66b & 24b^2 & 0 & 39b & -18b^2 & 0 & -39b & 18b^2 & 0 \\ 42c & 0 & -28c^2 & -42c & 0 & 112c^2 & -21c & 0 & 56c^2 & 21c & 0 & -14c^2 \\ -102 & -39b & -21c & 102 & 39b & -21c & 276 & -66b & -42c & -276 & 66b & -42c \\ 39b & 18b^2 & 0 & -39b & -18b^2 & 0 & -66b & 24b^2 & 0 & 66b & -24b^2 & 0 \\ 21c & 0 & -14c^2 & -21c & 0 & 56c^2 & -42c & 0 & 112c^2 & 42c & 0 & -28c^2 \\ 102 & 39b & 21c & -102 & -39b & 21c & -276 & 66b & 42c & 276 & -66b & 42c \\ -39b & -18b^2 & 0 & 39b & 18b^2 & 0 & 66b & -24b^2 & 0 & -66b & 24b^2 & 0 \\ 21c & 0 & 56c^2 & -21c & 0 & -14c^2 & -42c & 0 & -28c^2 & 42c & 0 & 112c^2 \end{bmatrix} \tag{26}$$

$$\mathbf{M}_{y_e} = \frac{\rho hcb}{630} \times \begin{bmatrix} 276 & 42b & 66c & 102 & 21b & -39c & -102 & 21b & 39c & -276 & 42b & -66c \\ 42b & 112b^2 & 0 & 21b & 56b^2 & 0 & -21b & -14b^2 & 0 & -42b & -28b^2 & 0 \\ 66c & 0 & 24c^2 & 39c & 0 & -18c^2 & -39c & 0 & 18c^2 & -66c & 0 & -24c^2 \\ 102 & 21b & 39c & 276 & 42b & -66c & -276 & 42b & 66c & -102 & 21b & -39c \\ 21b & 56b^2 & 0 & 42b & 112b^2 & 0 & -42b & -28b^2 & 0 & -21b & -14b^2 & 0 \\ -39c & 0 & -18c^2 & -66c & 0 & 24c^2 & 66c & 0 & -24c^2 & 39c & 0 & 18c^2 \\ -102 & -21b & -39c & -276 & -42b & 66c & 276 & -42b & -66c & 102 & -21b & 39c \\ 21b & -14b^2 & 0 & 42b & -28b^2 & 0 & -42b & 112b^2 & 0 & -21b & 56b^2 & 0 \\ 39c & 0 & 18c^2 & 66c & 0 & -24c^2 & -66c & 0 & 24c^2 & -39c & 0 & -18c^2 \\ -276 & -42b & -66c & -102 & -21b & 39c & 102 & -21b & -39c & 276 & -42b & 66c \\ 42b & -28b^2 & 0 & 21b & -14b^2 & 0 & -21b & 56b^2 & 0 & -42b & 112b^2 & 0 \\ -66c & 0 & -24c^2 & -39c & 0 & 18c^2 & 39c & 0 & -18c^2 & 66c & 0 & 24c^2 \end{bmatrix} \tag{27}$$

For the special case when the plate is local, the mass matrix derived above reduces to the classical mass matrix as $e_0 a = 0$ [43].

Based on the discussions in this section for all the three systems considered here, in general the element mass matrix of a nonlocal dynamic system can be expressed as

$$\mathbf{M}_e = \mathbf{M}_{0_e} + \mathbf{M}_{\mu_e} \tag{28}$$

Here $\mathbf{M}_{0_e}$ is the element stiffness matrix corresponding to the underlying local system and $\mathbf{M}_{\mu_e}$ is the additional term arising due to the nonlocal effect.

3. Modal analysis of nonlocal dynamical systems

Modal analysis is a classical technique developed by Rayleigh [45] in 1877. Contemporary methods for damped multi body dynamic systems [38,39,46] essentially rely on this classical approach. Here we employ the classical modal analysis in conjunction with the first-order perturbation method, also pioneered by Rayleigh, to nonlocal dynamic system. Using the finite element formulation, the stiffness matrix of the local and nonlocal system turns out to be identical to each other. The mass matrix of the nonlocal system is however different from its equivalent local counterpart. Assembling the element matrices and applying the boundary conditions, following the usual procedure of the finite element method [47] one obtains the global mass matrix as

$$\mathbf{M} = \mathbf{M}_0 + \mathbf{M}_\mu \tag{29}$$

In the above equation $\mathbf{M}_0$ is the usual global mass matrix arising in the conventional local system and $\mathbf{M}_\mu$ is matrix arising due to nonlocal nature of the systems. In general we can express this matrix by

$$\mathbf{M}_\mu = \left(\frac{e_0 a}{L}\right)^2 \widehat{\mathbf{M}}_\mu \tag{30}$$

where $\widehat{\mathbf{M}}_\mu$ is a nonnegative definite matrix. The matrix $\mathbf{M}_\mu$ is therefore, a scale-dependent matrix and its influence reduces if the length of the system L is large compared to the parameter $e_0 a$. Majority of the current finite element software and other computational tools do not explicitly consider the nonlocal part of the mass matrix. For the design and analysis of future generation of nanoelectromechanical systems it is vitally important to consider the nonlocal influence. In this section we are interested in understanding the impact of the difference in the mass matrix on the dynamic characteristics of the system. In particular the following questions of fundamental interest have been addressed:

- Under what condition a nonlocal system possess classical local normal modes?
- How the vibration modes and frequencies of a nonlocal system can be understood in the light of the results from classical local systems?

By addressing these questions, it would be possible to extend conventional 'local' elasticity based finite element software to analyse nonlocal systems arising in the modelling of complex nanoscale built-up structures.

3.1. Conditions for classical normal modes

The equation of motion of a discretised nonlocal damped system with n degrees of freedom can be expressed as

$$[\mathbf{M}_0 + \mathbf{M}_\mu]\ddot{\mathbf{u}}(t) + \mathbf{C}\dot{\mathbf{u}}(t) + \mathbf{K}\mathbf{u}(t) = \mathbf{f}(t) \tag{31}$$

Here $\mathbf{u}(t) \in \mathbb{R}^n$ is the displacement vector, $\mathbf{f}(t) \in \mathbb{R}^n$ is the forcing vector, $\mathbf{K}, \mathbf{C} \in \mathbb{R}^{n\times n}$ are respectively the global stiffness and the viscous damping matrix. In general $\mathbf{M}_0$ and $\mathbf{M}_\mu$ are positive definite symmetric matrices, $\mathbf{C}$ and $\mathbf{K}$ are non-negative definite symmetric matrices. The equation of motion of corresponding local system is given by

$$\mathbf{M}_0\ddot{\mathbf{u}}_0(t) + \mathbf{C}\dot{\mathbf{u}}_0(t) + \mathbf{K}\mathbf{u}_0(t) = \mathbf{f}(t) \tag{32}$$

where $\mathbf{u}_0(t) \in \mathbb{R}^n$ is the local displacement vector. The natural frequencies ($\omega_j \in \mathbb{R}$) and the mode shapes ($\mathbf{x}_j \in \mathbb{R}^n$) of the corresponding undamped local system can be obtained by solving the matrix eigenvalue problem [38] as

$$\mathbf{K}\mathbf{x}_j = \omega_j^2 \mathbf{M}_0 \mathbf{x}_j, \quad \forall\, j = 1, 2, \ldots, n \tag{33}$$

The undamped local eigenvectors satisfy an orthogonality relationship over the local mass and stiffness matrices, that is

$$\mathbf{x}_k^T \mathbf{M}_0 \mathbf{x}_j = \delta_{kj} \tag{34}$$

and

$$\mathbf{x}_k^T \mathbf{K} \mathbf{x}_j = \omega_j^2 \delta_{kj}, \quad \forall\, k, j = 1, 2, \ldots, n \tag{35}$$

where δ_{kj} is the Kroneker delta function. We construct the local modal matrix

$$\mathbf{X} = [\mathbf{x}_1, \mathbf{x}_2, \ldots, \mathbf{x}_n] \in \mathbb{R}^n \tag{36}$$

The local modal matrix can be used to diagonalize the local system (32) provided the damping matrix $\mathbf{C}$ is simultaneously diagonalisable with $\mathbf{M}_0$ and $\mathbf{K}$. This condition, known as the proportional damping, originally introduced by Rayleigh [45] in

1877, is still in wide use today. The mathematical condition for proportional damping can be obtained from the commutative behaviour of the system matrices [48]. This can be expressed as

$$\mathbf{C}\mathbf{M}_0^{-1}\mathbf{K} = \mathbf{K}\mathbf{M}_0^{-1}\mathbf{C} \tag{37}$$

or equivalently $\mathbf{C} = \mathbf{M}_0 f(\mathbf{M}_0^{-1}\mathbf{K})$ as shown in [49].

Considering undamped nonlocal system and premultiplying the equation by $\mathbf{M}_0^{-1}$ we have

$$(\mathbf{I}_n + \mathbf{M}_0^{-1}\mathbf{M}_\mu)\ddot{\mathbf{u}}(t) + (\mathbf{M}_0^{-1}\mathbf{K})\mathbf{u}(t) = \mathbf{M}_0^{-1}\mathbf{f}(t) \tag{38}$$

This system can be diagonalised by a similarity transformation which also diagonalise $(\mathbf{M}_0^{-1}\mathbf{K})$ provided the matrices $(\mathbf{M}_0^{-1}\mathbf{M}_\mu)$ and $(\mathbf{M}_0^{-1}\mathbf{K})$ commute. This implies that the condition for existence of classical local normal modes is

$$(\mathbf{M}_0^{-1}\mathbf{K})(\mathbf{M}_0^{-1}\mathbf{M}_\mu) = (\mathbf{M}_0^{-1}\mathbf{M}_\mu)(\mathbf{M}_0^{-1}\mathbf{K}) \tag{39}$$

or

$$\mathbf{K}\mathbf{M}_0^{-1}\mathbf{M}_\mu = \mathbf{M}_\mu\mathbf{M}_0^{-1}\mathbf{K} \tag{40}$$

If the above condition is satisfied, then a nonlocal undamped system can be diagonalised by the classical local normal modes. However, it is also possible to have nonlocal normal modes which can diagonalize the nonlocal undamped system as discussed in the next subsection.

3.2. Nonlocal normal modes

Nonlocal normal modes can be obtained by the undamped nonlocal eigenvalue problem:

$$\mathbf{K}\mathbf{u}_j = \lambda_j^2[\mathbf{M}_0 + \mathbf{M}_\mu]\mathbf{u}_j, \quad \forall\, j = 1, 2, \ldots, n \tag{41}$$

Here λ_j and $\mathbf{u}_j$ are the nonlocal natural frequencies and nonlocal normal modes of the system. We can define a nonlocal modal matrix:

$$\mathbf{U} = [\mathbf{u}_1, \mathbf{u}_2, \ldots, \mathbf{u}_n] \in \mathbb{R}^n \tag{42}$$

which will unconditionally diagonalize the nonlocal undamped system. It should be remembered that in general nonlocal normal modes and frequencies will be different from their local counterparts.

Under certain restrictive condition it may be possible to diagonalise the damped nonlocal system using classical normal modes. Premultiplying the equation of motion (31) by $\mathbf{M}_0^{-1}$, the required condition is that $(\mathbf{M}_0^{-1}\mathbf{M}_\mu)$, $(\mathbf{M}_0^{-1}\mathbf{C})$ and $(\mathbf{M}_0^{-1}\mathbf{K})$ must commute pairwise. This implies that in addition to the two conditions given by Eqs. (37) and (40), we also need a third condition:

$$\mathbf{C}\mathbf{M}_0^{-1}\mathbf{M}_\mu = \mathbf{M}_\mu\mathbf{M}_0^{-1}\mathbf{C} \tag{43}$$

If we consider the diagonalisation of the nonlocal system by the nonlocal modal matrix in (42), then the concept of proportional damping can be applied similar to that of the local system. One can obtain the required condition similar to Caughey's condition [48] as in Eq. (37) by replacing the mass matrix with $\mathbf{M}_0 + \mathbf{M}_\mu$. If this condition is satisfied, then the equation of motion can be diagonalised by the nonlocal normal modes and in general not by the classical normal modes.

3.3. Approximate nonlocal normal modes

Majority of the existing finite element software calculate the classical normal modes. However, it was shown that only under certain restrictive condition, the classical normal modes can be used to diagonalise the system. In general one need to use nonlocal normal modes to diagonalise the equation of motion (31), which is necessary for efficient dynamic analysis and physical understanding of the system. In this section we aim to express nonlocal normal modes in terms of classical normal modes. Since the classical normal modes are well understood, this approach will allow us to develop physical understanding of the nonlocal normal modes. The analytical approach adopted here is motivated by the first-order perturbation method used for complex modes arising in non-proportionally damped dynamic systems. We refer to the book by Rayleigh [45] for viscously damped systems and a more recent book [46] on general non-viscously damped systems for more detailed discussions.

For distinct undamped eigenvalues (ω_l^2), local eigenvectors $\mathbf{x}_l$, $\forall\, l = 1, \ldots, n$, form a complete set of vectors. For this reason each nonlocal normal mode $\mathbf{u}_j$ can be expanded as a linear combination of $\mathbf{x}_l$. Thus, an expansion of the form:

$$\mathbf{u}_j = \sum_{l=1}^{n} \alpha_l^{(j)}\mathbf{x}_l \tag{44}$$

may be considered. Without any loss of generality, we can assume that $\alpha_j^{(j)}=1$ (normalisation) which leaves us to determine $\alpha_l^{(j)}, \forall l\neq j$. Substituting the expansion of $\mathbf{u}_j$ into the eigenvalue equation (41), one obtains

$$[-\lambda_j^2(\mathbf{M}_0+\mathbf{M}_\mu)+\mathbf{K}]\sum_{l=1}^{n}\alpha_l^{(j)}\mathbf{x}_l=\mathbf{0} \tag{45}$$

For the case when $\alpha_l^{(j)}$ are approximate, the error involving the projection in Eq. (44) can be expressed as

$$\boldsymbol{\varepsilon}_j=\sum_{l=1}^{n}[-\lambda_j^2(\mathbf{M}_0+\mathbf{M}_\mu)+\mathbf{K}]\alpha_l^{(j)}\mathbf{x}_l \tag{46}$$

We use a Galerkin approach to minimise this error by viewing the expansion as a projection in the basis functions $\mathbf{x}_l\in\mathbb{R}^n, \forall l=1,2,\ldots n$. Therefore, making the error orthogonal to the basis functions one has

$$\boldsymbol{\varepsilon}_j\perp\mathbf{x}_l \quad \text{or} \quad \mathbf{x}_k^T\boldsymbol{\varepsilon}_j=0 \quad \forall\, k=1,2,\ldots,n \tag{47}$$

Using the orthogonality property of the undamped local modes described by Eqs. (34) and (35) one obtains

$$\sum_{l=1}^{n}[-\lambda_j^2(\delta_{kl}+M'_{\mu_{kl}})+\omega_k^2\delta_{kl}]\alpha_l^{(j)}=0 \tag{48}$$

where $M'_{\mu_{kl}}=\mathbf{x}_k^T\mathbf{M}_\mu\mathbf{x}_l$ are the elements of the nonlocal part of the modal mass matrix. The j-th equation of this set obtained by setting $k=j$ and can be written as

$$-\lambda_j^2(1+M'_{\mu_{jj}})+\omega_j^2-\lambda_j^2\sum_{l\neq j}^{n}(M'_{\mu_{jl}})\alpha_l^{(j)}=0 \tag{49}$$

Assuming that the off-diagonal terms of the nonlocal part of the modal mass matrix are small and $\alpha_l^{(j)}\ll 1, \forall l\neq j$, approximate nonlocal frequencies can be obtained as

$$\lambda_j\approx\frac{\omega_j}{\sqrt{1+M'_{\mu_{jj}}}} \tag{50}$$

This equation gives a closed-form expression relating nonlocal natural frequencies λ_j and local natural frequencies ω_j. If the length-scale parameter is large, then diagonal elements of the nonlocal part of the modal mass matrix becomes smaller and consequently the nonlocal frequencies approach the classical local frequencies. Eq. (50) can also be viewed as a general correction to the local frequencies due to the nonlocal effect arising due to small length scale.

For the general case when $k\neq j$, from Eq. (48) we have

$$[-\lambda_j^2(1+M'_{\mu_{kk}})+\omega_k^2]\alpha_k^{(j)}-\lambda_j^2\sum_{l\neq k}^{n}(M'_{\mu_{kl}})\alpha_l^{(j)}=0 \tag{51}$$

Recalling that $\alpha_j^{(j)}=1$, this equation can be expressed as

$$[-\lambda_j^2(1+M'_{\mu_{kk}})+\omega_k^2]\alpha_k^{(j)}=\lambda_j^2\left[M'_{\mu_{kj}}+\sum_{l\neq k\neq j}^{n}M'_{\mu_{kl}}\alpha_l^{(j)}\right] \tag{52}$$

Again assuming that the off-diagonal terms of the nonlocal part of the modal mass matrix are small and $\alpha_l^{(j)}\ll 1, \forall l\neq j$, we can obtain

$$\alpha_k^{(j)}\approx\frac{\lambda_j^2\,M'_{\mu_{kj}}}{-\lambda_j^2(1+M'_{\mu_{kk}})+\omega_k^2}\approx\frac{\lambda_j^2}{(\lambda_k^2-\lambda_j^2)}\frac{M'_{\mu_{kj}}}{(1+M'_{\mu_{kk}})} \tag{53}$$

Substituting this in the original expansion (44), the nonlocal normal modes can be expressed in terms of the classical normal modes as

$$\mathbf{u}_j\approx\mathbf{x}_j+\left\{\sum_{k\neq j}^{n}\frac{\lambda_j^2}{(\lambda_k^2-\lambda_j^2)}\frac{M'_{\mu_{kj}}}{(1+M'_{\mu_{kk}})}\mathbf{x}_k\right\} \tag{54}$$

This equation explicitly relates nonlocal normal modes with the classical normal modes. From this expression, the following insights about the nonlocal normal modes can be deduced:

- Each nonlocal mode can be viewed as a sum of two principal components. One of them is parallel to the corresponding local mode and the other is mass-orthogonal to it as all $\mathbf{x}_k$ are mass-orthogonal to $\mathbf{x}_j$ for $j\neq k$.
- Due to the term $(\lambda_k^2-\lambda_j^2)$ in the denominator, for a given nonlocal mode, only few adjacent local modes contributes to the mass-orthogonal component.
- For systems with well separated natural frequencies, the contribution of the mass-orthogonal component becomes smaller compared to the parallel component.

Eqs. (50) and (54) completely define the nonlocal natural frequencies and mode shapes in terms of the local natural frequencies and mode shapes. Accuracy of these expressions will be investigated through numerical examples in Section examples. Dynamic response of nonlocal damped systems is considered next.

4. Dynamic response of damped nonlocal systems

Forced response of damped nonlocal systems in the frequency domain is considered. Assuming that all the initial conditions are zero and taking the Fourier transformation of the equation of motion (31) we have

$$\mathbf{D}(\mathrm{i}\omega)\overline{\mathbf{u}}(\mathrm{i}\omega)=\overline{\mathbf{f}}(\mathrm{i}\omega) \tag{55}$$

where the nonlocal dynamic stiffness matrix is given by

$$\mathbf{D}(\mathrm{i}\omega)=-\omega^2[\mathbf{M}_0+\mathbf{M}_\mu]+\mathrm{i}\omega\mathbf{C}+\mathbf{K} \tag{56}$$

In Eq. (55) $\overline{\mathbf{u}}(\mathrm{i}\omega)$ and $\overline{\mathbf{f}}(\mathrm{i}\omega)$ are respectively the Fourier transformations of the response and the forcing vectors. Using the local modal matrix (36), the dynamic stiffness matrix can be transformed to the modal coordinate as

$$\mathbf{D}'(\mathrm{i}\omega)=\mathbf{X}^T\mathbf{D}(\mathrm{i}\omega)\mathbf{X}=-\omega^2[\mathbf{I}+\mathbf{M}'_\mu]+\mathrm{i}\omega\mathbf{C}'+\boldsymbol{\Omega}^2 \tag{57}$$

where $\mathbf{I}$ is a n-dimensional identity matrix, $\boldsymbol{\Omega}^2$ is a diagonal matrix containing the squared local natural frequencies and $(\bullet)'$ denotes that the quantity is in the modal coordinates. Unless all the conditions derived in Section nonlocalmodes are satisfied, in general $\mathbf{M}'_\mu$ and $\mathbf{C}'$ are not diagonal matrices. We separate the diagonal and off-diagonal terms of these matrices and rewrite Eq. (57) as

$$\mathbf{D}'(\mathrm{i}\omega)=\underbrace{-\omega^2\left[\mathbf{I}+\overline{\mathbf{M}}'_\mu\right]+\mathrm{i}\omega\overline{\mathbf{C}}'+\boldsymbol{\Omega}^2}_{\text{diagonal}}+\underbrace{\left(-\omega^2\Delta\mathbf{M}'_\mu+\mathrm{i}\omega\Delta\mathbf{C}'\right)}_{\text{off}-\text{diagonal}} \tag{58}$$

$$=\overline{\mathbf{D}}'(\mathrm{i}\omega)+\Delta\mathbf{D}'(\mathrm{i}\omega) \tag{59}$$

From Eq. (55) the dynamic response of the system can be obtained as

$$\overline{\mathbf{u}}(\mathrm{i}\omega)=\mathbf{H}(\mathrm{i}\omega)\overline{\mathbf{f}}(\mathrm{i}\omega)=\left[\mathbf{X}\mathbf{D}'^{-1}(\mathrm{i}\omega)\mathbf{X}^T\right]\overline{\mathbf{f}}(\mathrm{i}\omega) \tag{60}$$

where the matrix $\mathbf{H}(\mathrm{i}\omega)$ is known as the transfer function matrix. From the expression of the modal dynamic stiffness matrix in Eq. (59) we have

$$\mathbf{D}'^{-1}(\mathrm{i}\omega)=\left[\overline{\mathbf{D}}'(\mathrm{i}\omega)\left(\mathbf{I}+\overline{\mathbf{D}}'^{-1}(\mathrm{i}\omega)\Delta\mathbf{D}'(\mathrm{i}\omega)\right)\right]^{-1} \tag{61}$$

$$\approx\overline{\mathbf{D}}'^{-1}(\mathrm{i}\omega)-\overline{\mathbf{D}}'^{-1}(\mathrm{i}\omega)\Delta\mathbf{D}'(\mathrm{i}\omega)\overline{\mathbf{D}}'^{-1}(\mathrm{i}\omega) \tag{62}$$

In the above equation the diagonal part $\overline{\mathbf{D}}'^{-1}(\mathrm{i}\omega)$ is expected to be the dominant term and its elements can be expressed as

$$\left\{\overline{\mathbf{D}}'^{-1}(\mathrm{i}\omega)\right\}_{jj}=\frac{1}{-\omega^2\left(1+M'_{\mu_{jj}}\right)+2\mathrm{i}\omega\omega_j\zeta_j+\omega_j^2} \tag{63}$$

In the above we defined the modal damping factors as

$$\left\{\overline{\mathbf{C}}'\right\}_{jj}=2\omega_j\zeta_j \tag{64}$$

Substituting the approximate expression of $\mathbf{D}'^{-1}(\mathrm{i}\omega)$ from Eq. (62) into the expression of the transfer function matrix in Eq. (60) we have

$$\mathbf{H}(\mathrm{i}\omega)=\left[\mathbf{X}\mathbf{D}'^{-1}(\mathrm{i}\omega)\mathbf{X}^T\right]\approx\overline{\mathbf{H}}'(\mathrm{i}\omega)-\Delta\mathbf{H}'(\mathrm{i}\omega) \tag{65}$$

where

$$\overline{\mathbf{H}}'(\mathrm{i}\omega)=\mathbf{X}\overline{\mathbf{D}}'(\mathrm{i}\omega)\mathbf{X}^T=\sum_{k=1}^{n}\frac{\mathbf{x}_k\mathbf{x}_k^T}{-\omega^2\left(1+M'_{\mu_{kk}}\right)+2\mathrm{i}\omega\omega_k\zeta_k+\omega_k^2} \tag{66}$$

and

$$\Delta\mathbf{H}'(\mathrm{i}\omega)=\mathbf{X}\overline{\mathbf{D}}'^{-1}(\mathrm{i}\omega)\Delta\mathbf{D}'(\mathrm{i}\omega)\overline{\mathbf{D}}'^{-1}(\mathrm{i}\omega)\mathbf{X}^T \tag{67}$$

Considering that the matrix $\Delta\mathbf{D}'(\mathrm{i}\omega)$ has only off-diagonal terms, expanding the matrix multiplications a general term of the previous matrix can be expressed as

$$\Delta H'_{ij}(\mathrm{i}\omega) = \sum_{l=1}^{n}\sum_{k\neq l}^{n} \frac{x_{il}\Delta D'_{lk}(\mathrm{i}\omega)x_{jk}}{\left(-\omega^2(1+M'_{\mu_{ll}})+2\mathrm{i}\omega\omega_l\zeta_l+\omega_l^2\right)\left(-\omega^2(1+M'_{\mu_{kk}})+2\mathrm{i}\omega\omega_k\zeta_k+\omega_k^2\right)} \tag{68}$$

Eq. (65) therefore completely defines the transfer function of the damped nonlocal system in terms of the classical normal modes. This can be useful in practice as all the quantities arise in this expression can be obtained from a conventional finite element software. One only needs the nonlocal part of the mass matrix as derived in Section 2. Some notable features of the expression of the approximate transfer function matrix in Eq. (65) are

- For lightly damped systems, from Eq. (66) observe that the transfer function will have peaks around the nonlocal natural frequencies derived in the previous section. This justifies the consistency of the approximation used in the paper.
- The decomposition in Eq. (58) indicates that error in the transfer function depends on two components. They include the off-diagonal part of the modal nonlocal mass matrix $\Delta\mathbf{M}'_{\mu}$ and the off-diagonal part of the of the modal damping matrix $\Delta\mathbf{C}'$. While the error in the damping term is present for nonproportionally damped local systems, the error due to the nonlocal modal mass matrix in unique to the nonlocal system.
- For a proportionally damped system $\Delta\mathbf{C}'=\mathbf{O}$. For this case, error in the transfer function only depends on $\Delta\mathbf{M}'_{\mu}$.
- In general, error in the transfer function is expected to be higher for higher frequencies as both $\Delta\mathbf{C}'$ and $\Delta\mathbf{M}'_{\mu}$ are weighted by frequency ω.

The expressions of the nonlocal natural frequencies (50), nonlocal normal modes (54) and the nonlocal transfer function matrix (65) allow us to understand the dynamic characteristic of a nonlocal system in a qualitative and quantitative manner in the light of equivalent local systems. Next we illustrate these new expressions by numerical examples of nanoscale structures.

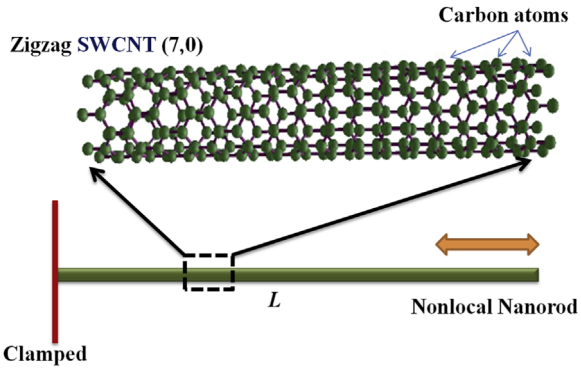

Fig. 4. Axial vibration of a zigzag (7, 0) single-walled carbon nanotube (SWCNT) with clamped-free boundary condition.

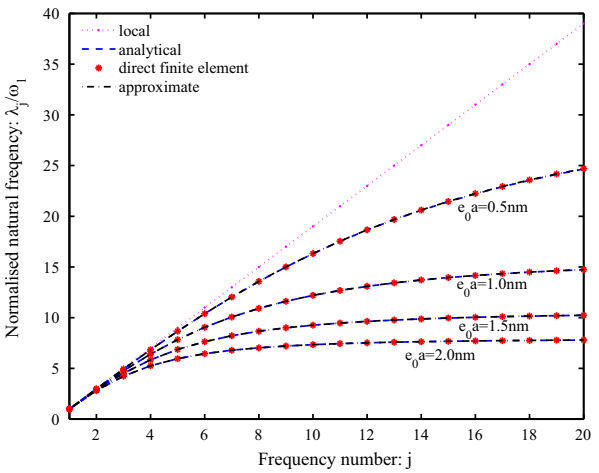

Fig. 5. The variation of first 20 undamped natural frequencies for the axial vibration of SWCNT. Four representative values of e_0a (in nm) are considered.

5. Numerical examples

5.1. Axial vibration of a single-walled carbon nanotube

A single-walled carbon nanotube (SWCNT) is considered to examine the accuracy of the nonlocal finite element formulation and approximate expressions of the natural frequencies, normal modes and transfer functions. A zigzag (7, 0) SWCNT with Young's modulus $E=6.85$ TPa, $L=25$ nm, density $\rho=9.517\times10^3$ kg/m^3 and thickness $t=0.08$ nm is taken from [27]. The system considered here is shown in Fig. 4. For a carbon nanotube with chirality (n_i, m_i), the diameter can be given by

$$d_i=\frac{r}{\pi}\sqrt{n_i^2+m_i^2+n_i m_i} \tag{69}$$

where $r=0.246$ nm. The diameter of the SWCNT shown in Fig. 4 is 0.55 nm. A constant modal damping factor of 1% for all the modes is assumed. By comparing with MD simulation results [50,51] it was observed that $e_0a=1$ nm is the optimal value of the nonlocal parameter. In this study however we consider a range of values of e_0a within 0–2 nm to understand its role on the accuracy of the dynamic characteristics of the system.

We consider clamped-free boundary condition for the SWCNT. Undamped nonlocal natural frequencies can be obtained [12] as

$$\lambda_j=\sqrt{\frac{EA}{m}}\frac{\sigma_j}{\sqrt{1+\sigma_j^2(e_0a)^2}},\quad \text{where}\quad \sigma_j=\frac{(2j-1)\pi}{2L},\quad j=1,2,\ldots \tag{70}$$

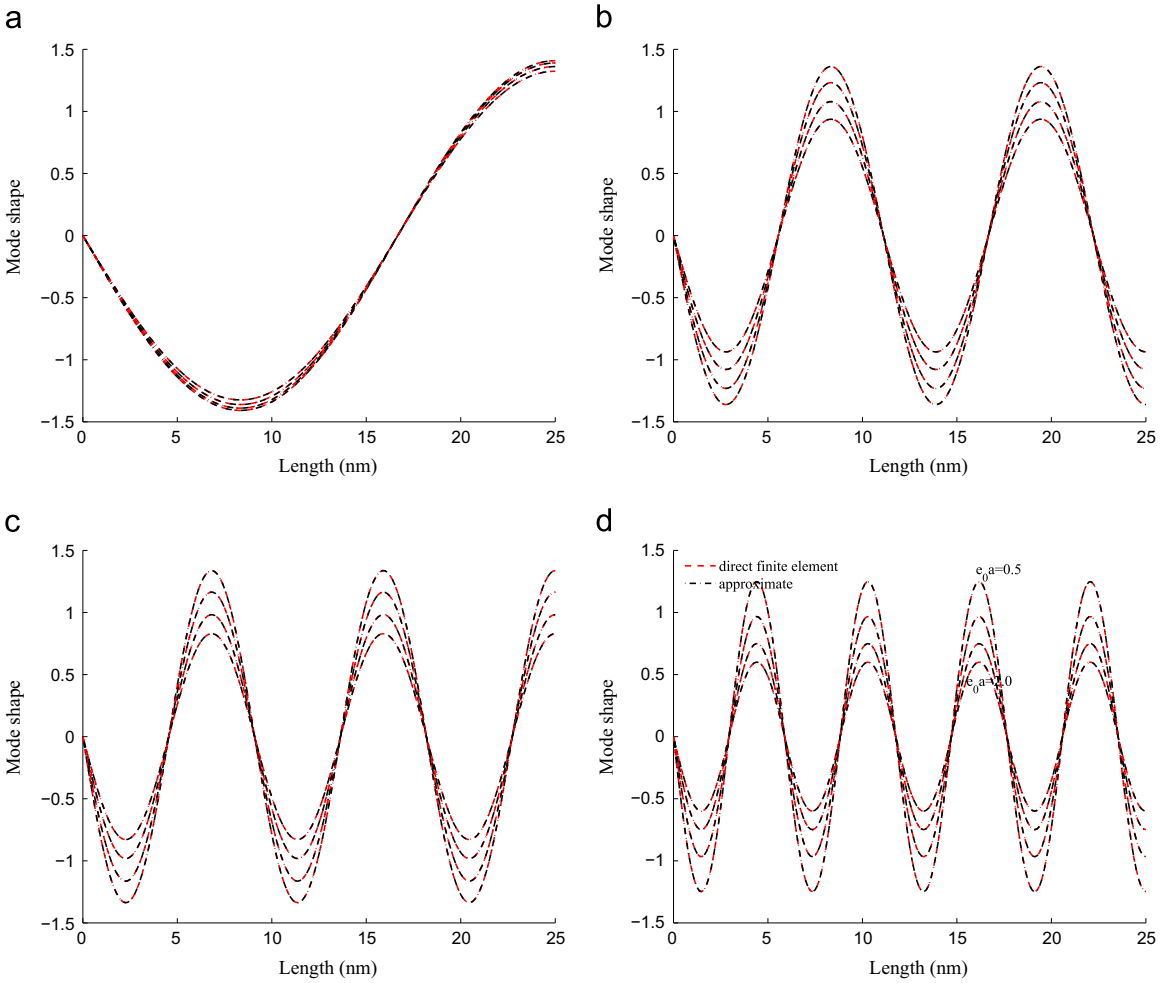

Fig. 6. Four selected mode shapes for the axial vibration of SWCNT. Exact finite element results are compared with the approximate analysis based on local eigensolutions. In each subplot four different values of e_0a, namely 0.5, 1.0, 1.5 and 2.0 nm have been used (see subplot d). (a) Mode 2, (b) Mode 5, (c) Mode 6, (d) Mode 9.

EA is the axial rigidity and m is the mass per unit length of the SWCNT. For the finite element analysis the SWCNT is divided into 200 elements. The dimension of each of the system matrices becomes 200×200, that is $n=200$. The global mass matrices $\mathbf{M}_0$ and $\mathbf{M}_\mu$ are obtained by assembling the element mass matrix given by (10). For this case it turns out (see element stiffness matrix in (9)) that the nonlocal part of the mass matrix is actually proportional to the stiffness matrix, that is $\mathbf{M}_\mu \propto \mathbf{K}$. Therefore, the condition for the existence of classical normal modes for the undamped system given by Eq. (40) is exactly satisfied in this case. This in turn implies that the error in the approximate expressions in Section 3.2 should be zero as $M_{\mu_{kl}} = 0, \forall k \neq l$. We give numerical results to demonstrate that the theory for the existence of classical normal modes for nonlocal system derived in Section 3.1 and the approximate expressions derived in Section 3.2 are consistent.

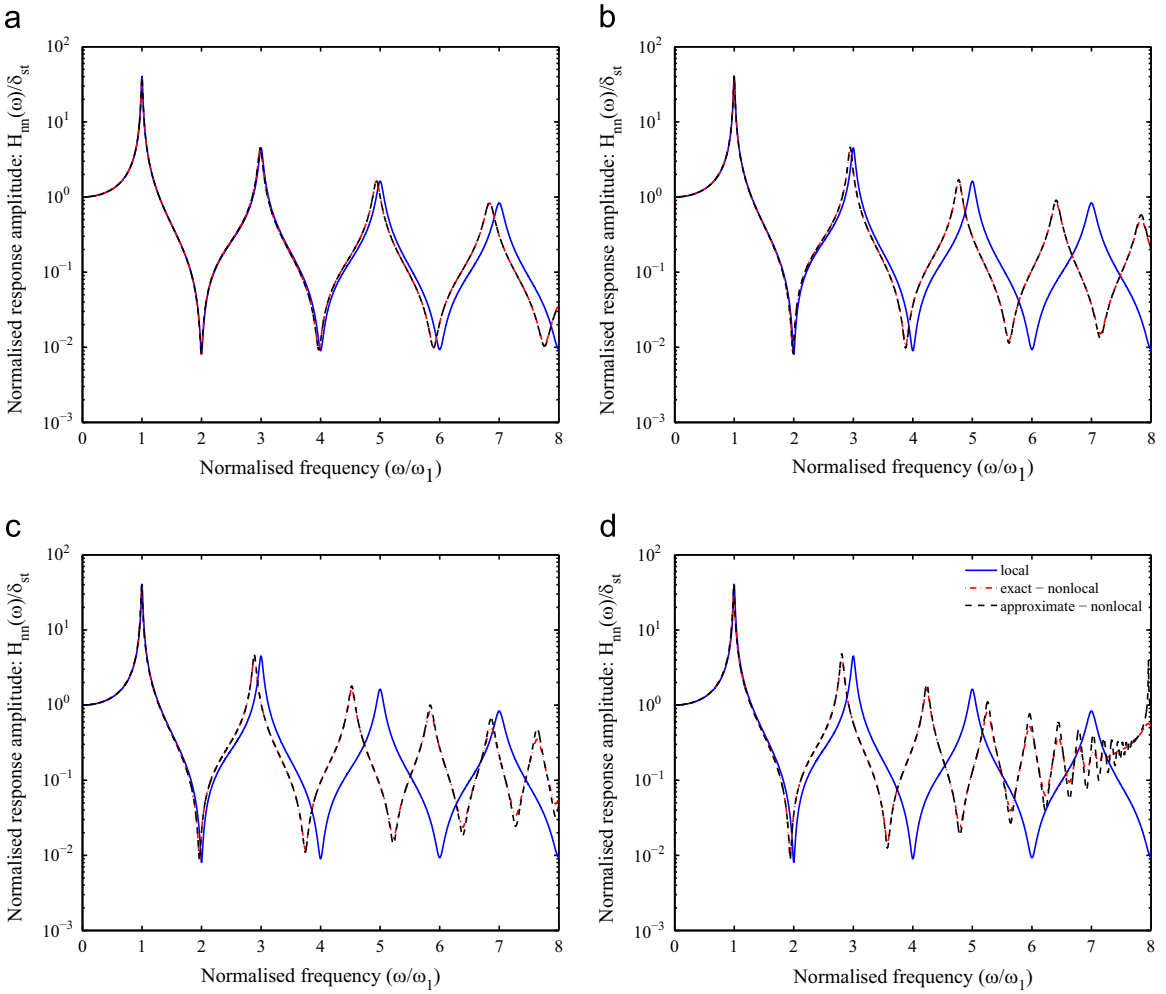

Fig. 7. Amplitude of the normalised frequency response of the SWCNT at the tip for different values of e_0a. Exact finite element results are compared with the approximate analysis based on local eigensolutions. (a) $e_0a = 0.5$ nm, (b) $e_0a = 1.0$ nm, (c) $e_0a = 1.5$ nm, (d) $e_0a = 2.0$ nm.

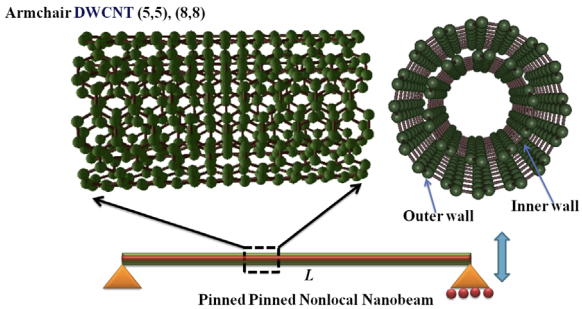

Fig. 8. Bending vibration of an armchair (5, 5), (8, 8) double-walled carbon nanotube (DWCNT) with pinned–pinned boundary condition.

In Fig. 5, the natural frequencies obtained using the analytical expression (70) are compared with direct finite element simulation results. The frequency values are normalised with respect to the first local natural frequency ω_1. First 20 nonlocal natural frequencies are shown and four values of e_0a, namely 0.5, 1.0, 1.5 and 2.0 nm have been used. In the same figure,

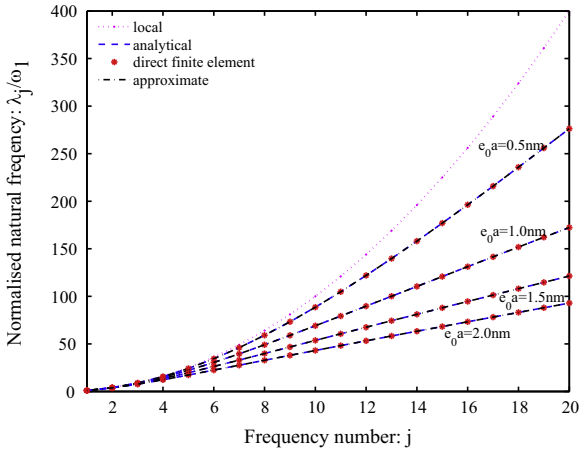

Fig. 9. The variation of first 20 undamped natural frequencies for the bending vibration of DWCNT. Four representative values of e_0a (in nm) are considered.

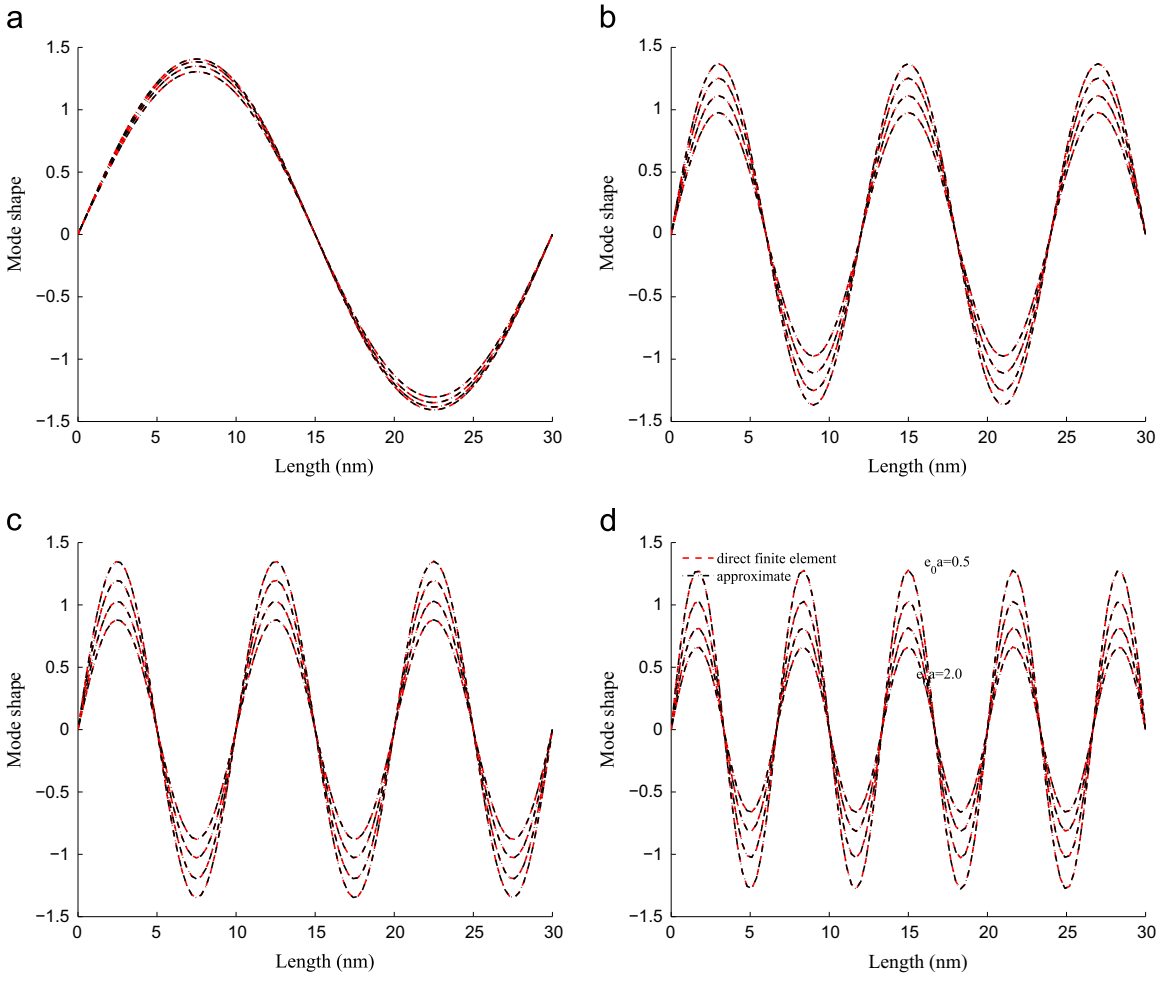

Fig. 10. Four selected mode shapes for the bending vibration of DWCNT. Exact finite element results are compared with the approximate analysis based on local eigensolutions. In each subplot four different values of e_0a, namely 0.5, 1.0, 1.5 and 2.0 nm have been used (see subplot d). (a) Mode 2, (b) Mode 5, (c) Mode 6, (d) Mode 9.

natural frequencies obtained using the direct finite element method and the results obtained using the approximate expression (50) are also shown. It can be observed that the values obtained using three different approaches coincide for this problem. Natural frequencies corresponding to the underlying local system is shown in Fig. 5. Local frequencies are qualitatively different from nonlocal frequencies as it increases linearly with the number of modes. Nonlocal frequencies on the other hand approaches to a constant value with increasing modes. This upper bound is known as the asymptotic frequency [35] and given by $\lambda_{\max} = 1/(e_0 a)\sqrt{EA/m}$. It is worth noting that the approximate expression of the natural frequency given by Eq. (50) is able to capture the asymptotic frequency for the axial vibration of SWCNT. Therefore, Eq. (50) can be used to understand both quantitative and qualitative behaviour of the natural frequencies of a nonlocal system.

In Fig. 6 mode shapes corresponding to modes 2, 5, 6 and 9 are shown for four values of the nonlocal parameter. These mode numbers are selected for illustration only. The results obtained from the direct finite element are compared with the approximate expression given by Eq. (54). The mode shapes obtained by both approaches agree each other well.

Finally in Fig. 7 the frequency response function of the tip of the SWCNT is shown for the four representative values of the nonlocal parameter. In the x-axis, excitation frequency normalised with respect to the first local frequency is considered. The frequency response is normalised by the static response δ_{st} (response when the excitation frequency is zero). The frequency response function of the underlying local model is also plotted to show the difference between the local and nonlocal responses. For the nonlocal system, the frequency response is obtained by the direct finite element method and the approximation derived in Section 4. As proportional damping model is assumed, the off-diagonal part of the modal damping matrix is a null matrix. For this case the approximate solution match exactly to the results obtained from the direct finite element method.

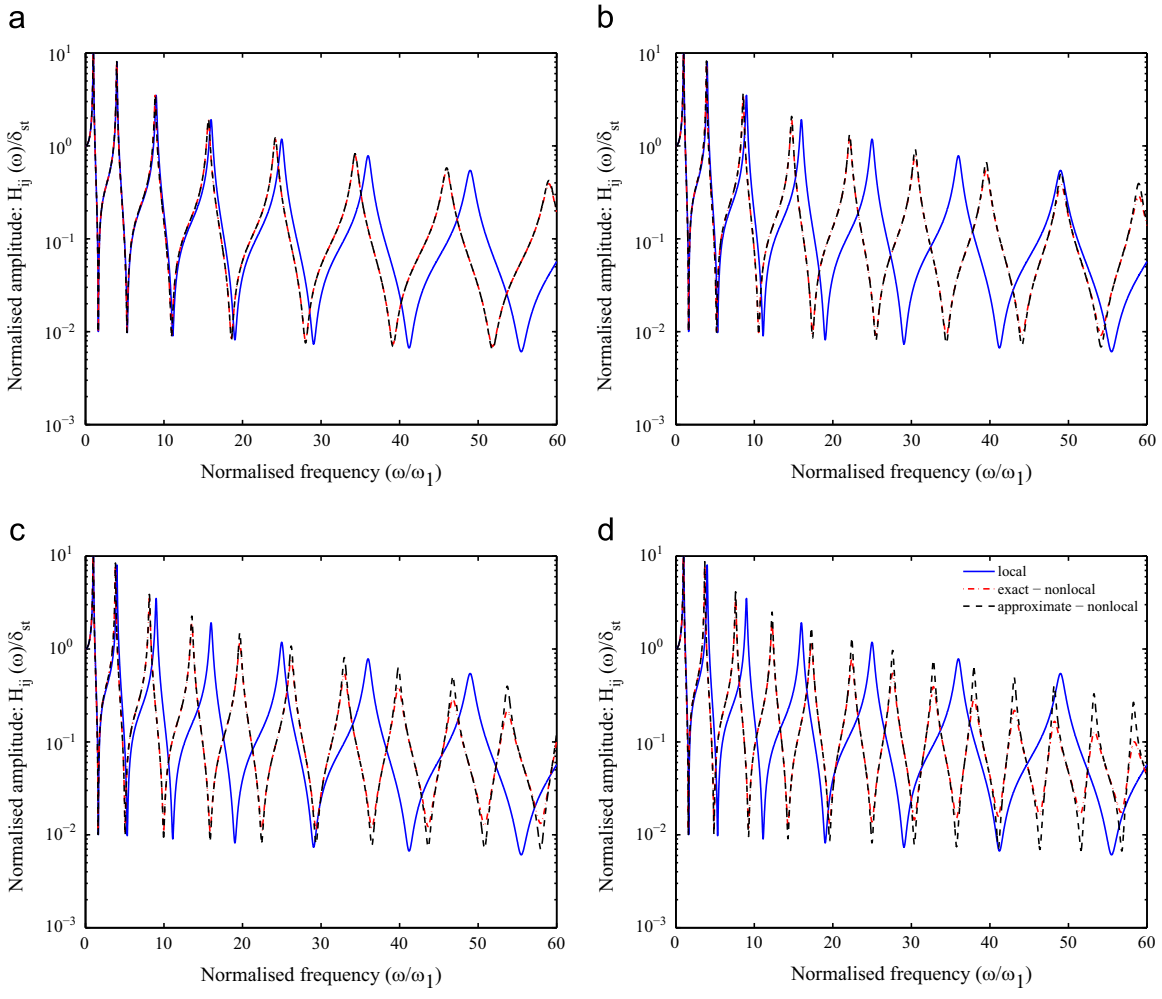

Fig. 11. Amplitude of the normalised frequency response of the DWCNT $H_{ij}(\omega)$ for $i=6, j=8$ for different values of $e_0 a$. Exact finite element results are compared with the approximate analysis based on local eigensolutions. (a) $e_0 a = 0.5$ nm, (b) $e_0 a = 1.0$ nm, (c) $e_0 a = 1.5$ nm, (d) $e_0 a = 2.0$ nm.

5.2. Bending vibration of a double-walled carbon nanotube

A double-walled carbon nanotube (DWCNT) is considered to examine the bending vibration characteristics. An armchair (5, 5), (8, 8) DWCNT with Young's modulus $E=1.0$ TPa, $L=30$ nm, density $\rho=2.3\times10^3$ kg/m^3 and thickness $t=0.35$ nm is considered as in [52]. The inner and the outer diameters of the DWCNT are respectively 0.68 nm and 1.1 nm. The system considered here is shown in Fig. 8 . We consider pinned–pinned boundary condition for the DWCNT. Undamped nonlocal natural frequencies can be obtained [12] as

$$\lambda_j=\sqrt{\frac{EI}{m}}\frac{\beta_j^2}{\sqrt{1+\beta_j^2(e_0a)^2}},\quad \text{where}\quad \beta_j=j\pi/L,\quad j=1,2,\ldots \tag{71}$$

EI is the bending rigidity and m is the mass per unit length of the DWCNT. For the finite element analysis the DWCNT is divided into 100 elements. The dimension of each of the system matrices become 200×200, that is $n=200$. The global mass matrices $\mathbf{M}_0$ and $\mathbf{M}_\mu$ are obtained by assembling the element mass matrix given by (15). Unlike the case of the axial vibration of rods, the nonlocal part of the mass matrix is not proportional to the stiffness matrix. Therefore, the condition for the existence of classical normal modes for the undamped system given by Eq. (40) is not satisfied for this case. This numerical study therefore quantifies the accuracy of the approximate expression proposed in the paper.

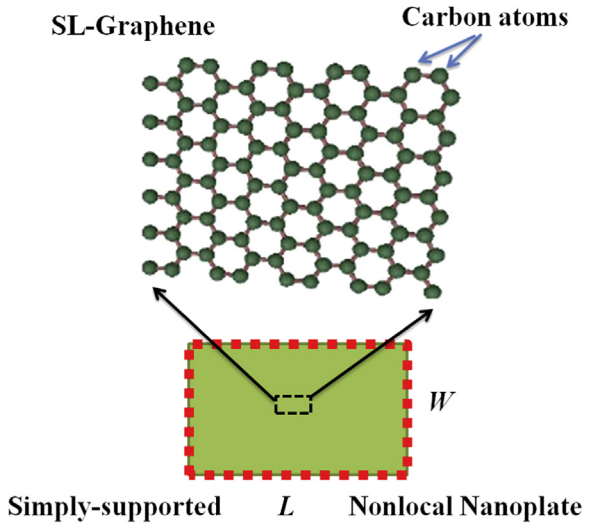

Fig. 12. Transverse vibration of a rectangular ($L=20$ nm, $W=15$ nm) single-layer graphene sheet (SLGS) with simply supported boundary condition along the four edges.

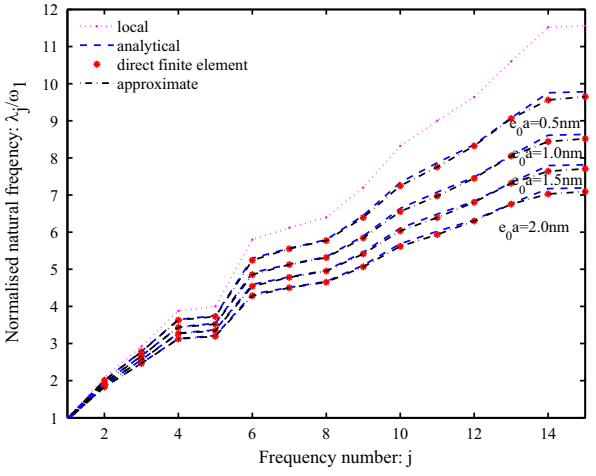

Fig. 13. The variation of first 15 undamped natural frequencies for the transverse vibration of SLGS. Four representative values of e_0a (in nm) are considered.

The natural frequencies obtained using the analytical expression (71) are compared with direct finite element simulation in Fig. 9. The frequency values are normalised with respect to the first local natural frequency. First 20 nonlocal natural frequencies are shown for four distinct values of e_0a, namely 0.5, 1.0, 1.5 and 2.0 nm. In the same figure, natural frequencies obtained using the direct finite element method and the results obtained using the approximate expression (50) are also shown. It can be observed that the values obtained using three different approaches almost coincide for this problem. Natural frequencies corresponding to the underlying local system is shown in Fig. 9. Local frequencies are qualitatively different from nonlocal frequencies as it increases quadratically with the number of modes. Nonlocal frequencies on the other hand increases linearly with the number of modes. The approximate expression of the natural frequency given by Eq. (50) is able to capture this crucial qualitative difference.

In Fig. 10 mode shapes corresponding to mode 2, 5, 6 and 9 are shown for four values of the nonlocal parameter. These mode numbers are selected for illustration only. The results obtained from the direct finite element is compared with the approximate expression given by Eq. (54). The mode shapes obtain by both approach agree to each other.

In Fig. 11 the amplitude of the frequency response function $H_{ij}(\omega)$ for $i=6, j=8$ is shown for the four representative values of the nonlocal parameter. In the x-axis, excitation frequency normalised with respect to the first local frequency is considered. The frequency response is normalise by the static response d_{st}. The frequency response function of the underlying local model is also plotted to show the difference between the local and nonlocal response. For the nonlocal system, the frequency response is obtained by the direct finite element method and the approximation derived in Section 4. As proportional damping model is assumed, the off-diagonal part of the modal damping matrix is a null matrix. For this case the approximate solution match closely to the results obtained from the direct finite element method. The dynamic response of the nonlocal system becomes very different from the corresponding local system for higher frequency values and higher values of the nonlocal parameter e_0a. The proposed approximate expression of the transfer function given in Eq. (65) can be used to understand this significant different behaviour for the bending vibration of DWCNT.

5.3. Transverse vibration of a single-layer graphene sheet

A rectangular single-layer graphene sheet (SLGS) is considered to examine the transverse vibration characteristics of nanoplates. The graphene sheet is of dimension $L=20$ nm, $W=15$ nm and Young's modulus $E=1.0$ TPa, density

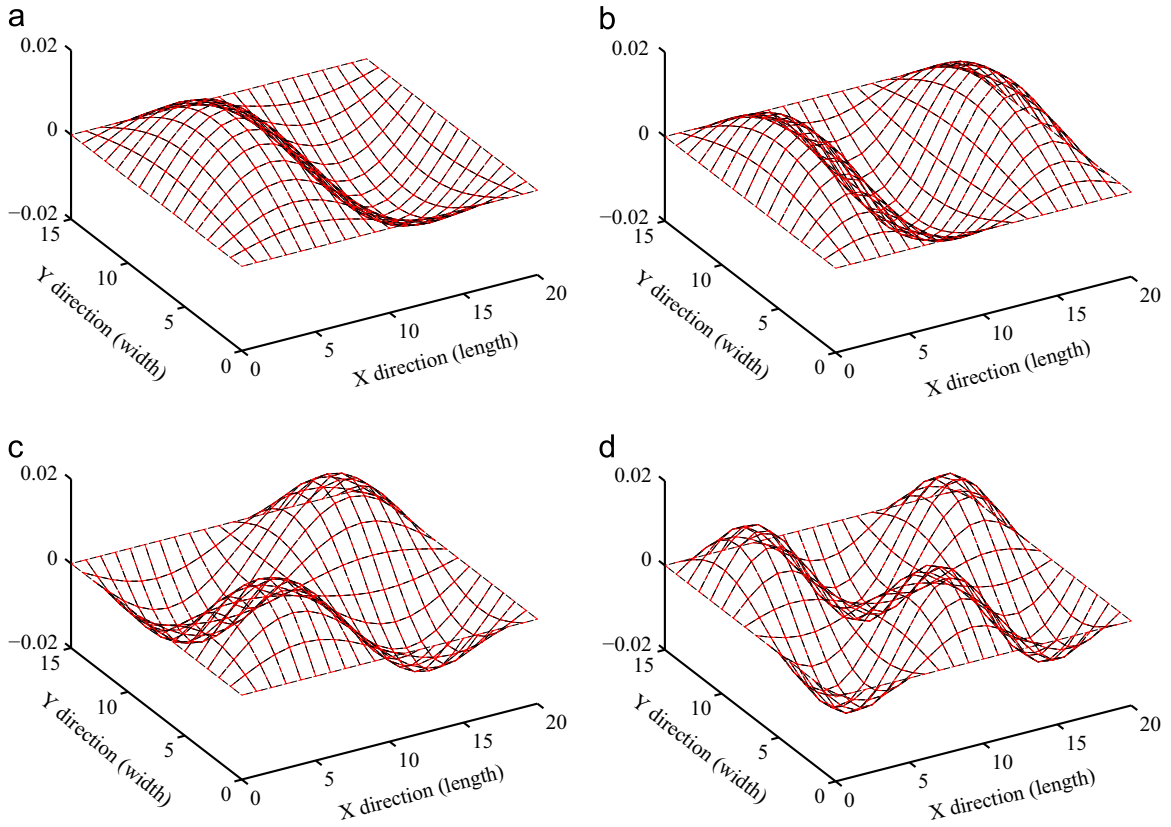

Fig. 14. Four selected mode shapes for the transverse vibration of SLGS for $e_0a=2$ nm. Exact finite element results (solid line) are compared with the approximate analysis based on local eigensolutions (dashed line). (a) Mode 2, (b) Mode 4, (c) Mode 5, (d) Mode 6.

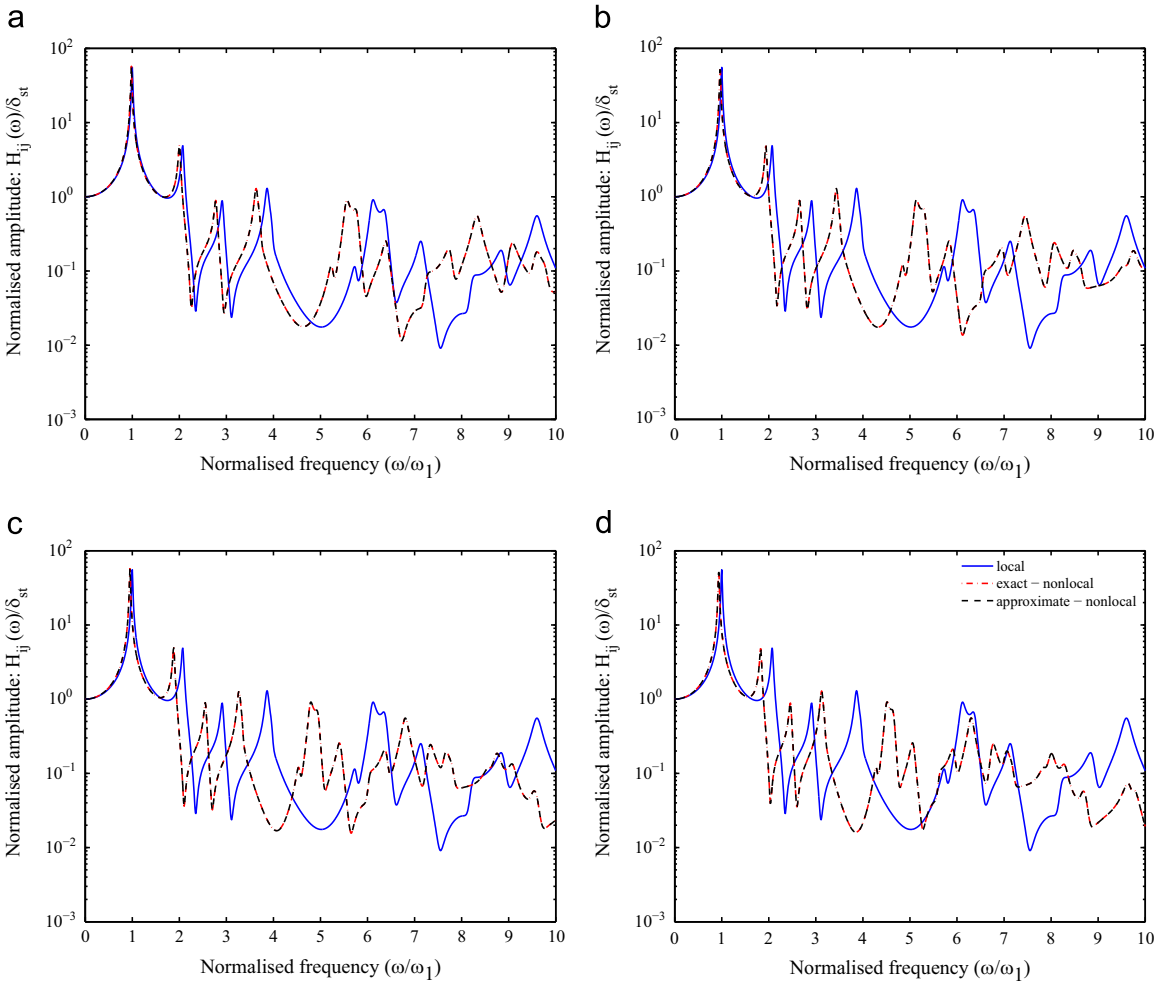

Fig. 15. Amplitude of the normalised frequency response $H_{ij}(\omega)$ for $i=475, j=342$ of the SLGS for different values of e_0a. Exact finite element results are compared with the approximate analysis based on local eigensolutions. (a) $e_0a=0.5$ nm, (b) $e_0a=1.0$ nm, (c) $e_0a=1.5$ nm, (d) $e_0a=2.0$ nm.

$\rho=2.25\times10^3$ kg/m^3, Poisson's ratio $\nu=0.3$ and thickness $h=0.34$ nm is considered as in [53]. The system considered here is shown in Fig. 12 . We consider simply supported boundary condition along the four edges for the SLGS. Undamped nonlocal natural frequencies can be obtained [54,44] as

$$\lambda_{ij}=\sqrt{\frac{D}{m}}\frac{\beta_{ij}^2}{\sqrt{1+\beta_{ij}^2(e_0a)^2}},\quad \text{where}\quad \beta_{ij}=\sqrt{(i\pi/L)^2+(j\pi/W)^2},\ \ i,j=1,2,\ldots \tag{72}$$

D is the bending rigidity and m is the mass per unit area of the SLGS. For the finite element analysis the DWCNT is divided into 20×15 elements. The dimension of each of the system matrices becomes 868×868, that is $n=868$. The global mass matrices $\mathbf{M}_0$ and $\mathbf{M}_\mu$ are obtained by assembling the element mass matrix given by (24). Like the case of the bending vibration of nanobeams, the nonlocal part of the mass matrix is not proportional to the stiffness matrix. Therefore, the condition for the existence of classical normal modes for the undamped system given by Eq. (40) is not satisfied for this case. Among the three types of systems considered here, only the nanorod satisfy the condition of existence of classical normal modes.

In Fig. 13, the natural frequencies obtained using the analytical expression (72) are compared with direct finite element simulation. The frequency values are normalised with respect to the first local natural frequency. First 15 nonlocal natural frequencies are shown for four distinct values of e_0a, namely 0.5, 1.0, 1.5 and 2.0 nm. In the same figure, natural frequencies obtained using the direct finite element method and the results obtained using the approximate expression (50) are also shown. It can be observed that the values obtained using three different approaches are very close. Natural frequencies corresponding to the underlying local system is shown in Fig. 13. Local frequencies diverge significantly from the nonlocal frequencies for higher frequency indices. The approximate expression of the natural frequency given by Eq. (50) is able to capture this quantitative difference very well.

In Fig. 14 mode shapes corresponding to mode 2, 4, 5, and 6 are shown when the nonlocal parameter $e_0a = 2$ nm. We have selected the highest value of e_0a as this leads to maximum inaccuracy of the proposed approximate expressions. Results obtained from the direct finite element and the approximate expression given by Eq. (54) are shown in these plots. These mode numbers are selected for illustration only. Results obtained from the direct finite element and the approximate expression given by Eq. (54) are shown in these plots. The mode shapes obtain by both approach agree to each other well.

Finally in Fig. 15 the amplitude of the frequency response function $H_{ij}(\omega)$ for $i = 475, j = 342$ is shown for the four representative values of the nonlocal parameter. In the x-axis, excitation frequency normalised with respect to the first local frequency is considered. The frequency response is normalise by the static response d_{st} (that is the response when the excitation frequency is zero rad/s). The frequency response function of the underlying local model is also plotted to show the difference between the local and nonlocal response. For the nonlocal system, the frequency response is obtained by the direct finite element method and the approximation derived in Section 4. As proportional damping model is assumed, the off-diagonal part of the modal damping matrix is a null matrix. For this case the approximate solution match exactly the results obtained from the direct finite element method. The dynamic response of the nonlocal system becomes very different from the corresponding local system for higher frequency values and higher values of the nonlocal parameter e_0a. The proposed approximate expression of the transfer function given in Eq. (65) can be used to understand this significant different behaviour.

6. Conclusions

Nonlocal elasticity is a promising theory for the modelling of nanoscale dynamical systems such as carbon nantotubes and graphene sheets. A finite element approach is proposed for dynamic analysis of general nonlocal structures. Explicit closed-form expressions of element mass and stiffness matrices of nanorods, nanobeams and nanoplates have been derived. The mass matrix can be decomposed into two parts, namely the classical local mass matrix $\mathbf{M}_0$ and a nonlocal part denoted by $\mathbf{M}_\mu$. The nonlocal part of the mass matrix is scale-dependent and vanishes for systems with large length-scale. Classical modal analysis in conjunction with first-order perturbation method is employed to understand the dynamic behaviour of general discrete nonlocal systems. Approximate expressions for nonlocal natural frequencies, mode shapes and frequency response functions have been derived. The main theoretical contributions made in this paper include the following results:

- An undamped nonlocal system will have classical normal modes provided the nonlocal part of the mass matrix satisfy the condition $\mathbf{K}\mathbf{M}_0^{-1}\mathbf{M}_\mu = \mathbf{M}_\mu\mathbf{M}_0^{-1}\mathbf{K}$ where $\mathbf{K}$ is the stiffness matrix.
- A viscously damped nonlocal system with damping matrix $\mathbf{C}$ will have classical normal modes provided $\mathbf{C}\mathbf{M}_0^{-1}\mathbf{K} = \mathbf{K}\mathbf{M}_0^{-1}\mathbf{C}$ and $\mathbf{C}\mathbf{M}_0^{-1}\mathbf{M}_\mu = \mathbf{M}_\mu\mathbf{M}_0^{-1}\mathbf{C}$ in addition to the previous condition.
- Natural frequency of a general nonlocal system can be expressed as $\lambda_j \approx \omega_j/\sqrt{1+M'_{\mu_{jj}}}$, $\forall j = 1, 2, \ldots$, where ω_j are the corresponding local frequencies and $M'_{\mu_{jj}}$ are the elements of nonlocal part of the mass matrix in the modal coordinate.
- Every nonlocal normal mode can be expressed as a sum of two principal components as

$$\mathbf{u}_j \approx \mathbf{x}_j + \left\{ \sum_{k \neq j}^{n} \frac{\lambda_j^2}{\left(\lambda_k^2 - \lambda_j^2\right)} \frac{M'_{\mu_{kj}}}{\left(1 + M'_{\mu_{kk}}\right)} \mathbf{x}_k \right\}, \forall j = 1, 2, \ldots.$$

  One of them is parallel to the corresponding local mode $\mathbf{x}_j$ and the other is mass-orthogonal to it.

The theoretical results obtained in the paper are applied to three representative problems, namely (a) axial vibration of a single-walled carbon nanotube, (b) bending vibration of a double-walled carbon nanotube, and (c) transverse vibration of a single-layer graphene sheet. These three systems are modelled by nonlocal rod, beam and plate respectively. Among these three systems, only the nonlocal rod model satisfy the condition of existence of classical normal modes. For the other two systems it was observed that the proposed approximate expressions of nonlocal natural frequencies, mode shapes and frequency response functions provide acceptable accuracy. The results obtained in the paper give physical insights into the dynamic behaviour of discrete nonlocal systems which can be understood in the light of well known dynamic behaviour of the underlying local systems.

Acknowledgements

S.A. acknowledges the support of Royal Society of London through the award of Wolfson Research Merit award.

References

[1] E. Wong, P. Sheehan, C. Lieber, Nanobeam mechanics: elasticity, strength, and toughness of nanorods and nanotubes, Science (1997) 277–1971.
[2] S. Iijima, T. Ichihashi, Single-shell carbon nanotubes of 1-nm diameter, Nature (1993) 363–603.
[3] J. Warner, F. Schaffel, M. Rummeli, B. Buchner, Examining the edges of multi-layer graphene sheets, Chem. Mater. (2009) 21–2418.
[4] D. Pacile, J. Meyer, C. Girit, A. Zettl, The two-dimensional phase of boron nitride: few-atomic-layer sheets and suspended membranes, Appl. Phys. Lett. (2008) 92.

[5] A. Brodka, J. Koloczek, A. Burian, Application of molecular dynamics simulations for structural studies of carbon nanotubes, J. Nanosci. Nanotechnol. (2007) 7–1505.
[6] B. Akgoz, O. Civalek, Strain gradient elasticity and modified couple stress models for buckling analysis of axially loaded micro-scaled beams, Int. J. Eng. Sci. 49 (11) (2011) 1268–1280.
[7] B. Akgoz, O. Civalek, Free vibration analysis for single-layered graphene sheets in an elastic matrix via modified couple stress theory, Materials & Design Mater. Des. 42 (2012) 164–171.
[8] E. Jomehzadeh, H. Noori, A. Saidi, The size-dependent vibration analysis of micro-plates based on a modified couple stress theory, Phys. E: Low-Dimens. Syst. Nanostruct. 43 (4) (2011) 877–883.
[9] M.H. Kahrobaiyan, M. Asghari, M. Rahaeifard, M. Ahmadian, Investigation of the size-dependent dynamic characteristics of atomic force microscope microcantilevers based on the modified couple stress theory, Int. J. Eng. Sci. 48 (12) (2010) 1985–1994.
[10] A.C. Eringen, On differential-equations of nonlocal elasticity and solutions of screw dislocation and surface waves, J. Appl. Phys. 54 (9) (1983) 4703–4710.
[11] J. Peddieson, G. Buchanan, R. McNitt, Application of nonlocal continuum models to nanotechnology, Int. J. Eng. Sci. 41 (3-5) (2003) 305–312.
[12] M. Aydogdu, Axial vibration of the nanorods with the nonlocal continuum rod model, Physica E 41 (5) (2009) 861–864.
[13] M. Aydogdu, Axial vibration analysis of nanorods (carbon nanotubes) embedded in an elastic medium using nonlocal elasticity, Mech. Res. Commun. 43 (2012) 34–40.
[14] T. Murmu, S. Adhikari, Nonlocal elasticity based vibration of initially pre-stressed coupled nanobeam systems, Eur. J. Mech.—A/Solids 34 (1) (2012) 52–62.
[15] T. Aksencer, M. Aydogdu, Levy type solution method for vibration and buckling of nanoplates using nonlocal elasticity theory, Phys. E: Low-Dimens. Syst. Nanostruct. 43 (4) (2011) 954–959.
[16] H. Babaei, A. Shahidi, Small-scale effects on the buckling of quadrilateral nanoplates based on nonlocal elasticity theory using the Galerkin method, Arch. Appl. Mech. 81 (8) (2011) 1051–1062.
[17] C.M. Wang, W.H. Duan, Free vibration of nanorings/arches based on nonlocal elasticity, J. Appl. Phys. 104 (2008) 014303:1-8.
[18] R. Artan, A. Tepe, Nonlocal effects in curved single-walled carbon nanotubes, Mech. Adv. Mater. Struct. 18 (5) (2011) 347–351.
[19] M. Aydogdu, S. Filiz, Modeling carbon nanotube-based mass sensors using axial vibration and nonlocal elasticity, Phys. E: Low-Dimens, Syst. Nanostruct. 43 (6) (2011) 1229–1234.
[20] R. Ansari, B. Arash, H. Rouhi, Vibration characteristics of embedded multi-layered graphene sheets with different boundary conditions via nonlocal elasticity, Compos. Struct. 93 (9) (2011) 2419–2429.
[21] T. Murmu, S.C. Pradhan, Vibration analysis of nano-single-layered graphene sheets embedded in elastic medium based on nonlocal elasticity theory, J. Appl. Phys. 105, 2009, 064319.
[22] J. Yang, X. Jia, S. Kitipornchai, Pull-in instability of nano-switches using nonlocal elasticity theory, J. Phys. D-Appl. Phys. 41(3), 2011, 035103.
[23] H. Heireche, A. Tounsi, H. Benhassaini, A. Benzair, M. Bendahmane, M. Missouri, S. Mokadem, Nonlocal elasticity effect on vibration characteristics of protein microtubules, Phys. E: Low-Dimens.Syst. Nanostruct. 42 (9) (2010) 2375–2379.
[24] C. Kiang, M. Endo, P. Ajayan, G. Dresselhaus, M. Dresselhaus, Size effects in carbon nanotubes, Phys. Rev. Lett. 81 (1998) 1869.
[25] C. Tang, L. Meng, L. Sun, K. Zhang, J. Zhong, Molecular dynamics study of ripples in graphene nanoribbons on 6 h-sic(0001): temperature and size effects, J. Appl. Phys. 104 (2008) 113536.
[26] B. Arash, Q. Wang, A review on the application of nonlocal elastic models in modeling of carbon nanotubes and graphenes, Comput. Mater. Sci. 51 (1) (2012) 303–313.
[27] T. Murmu, S. Adhikari, Nonlocal vibration of carbon nanotubes with attached buckyballs at tip, Mech. Res. Commun. 38 (1) (2011) 62–67.
[28] T. Murmu, S. Adhikari, Nonlocal effects in the longitudinal vibration of double-nanorod systems, Phys. E: Low-Dimens. Syst. Nanostruct. 43 (1) (2010) 415–422.
[29] S. Narendar, S. Gopalakrishnan, Axial wave propagation in coupled nanorod system with nonlocal small scale effects, Compos. Part B-Eng. 8142 (2013).
[30] J.K. Phadikar, S.C. Pradhan, Variational formulation and finite element analysis for nonlocal elastic nanobeams and nanoplates, Comput. Mater. Sci. 49 (3) (2010) 492–499.
[31] T. Murmu, S. Adhikari, Nonlocal vibration of bonded double-nanoplate-systems, Compos. Part B: Eng. 42 (7) (2011) 1901–1911.
[32] A.A. Pisano, A. Sofi, P. Fuschi, Nonlocal integral elasticity: 2d finite element based solutions, Int. J. Solids Struct. 46 (21) (2009) 3836–3849.
[33] T. Chang, Finite element analysis on vibration of nanorods with heterogeneous property and non-uniform cross section, Adv. Sci. Lett. 13 (1) (2012) 360–363.
[34] S. Narendar, S. Gopalakrishnan, Spectral finite element formulation for nanorods via nonlocal continuum mechanics, J. Appl. Mech.-Trans. ASME 78.
[35] S. Adhikari, T. Murmu, M. McCarthy, Dynamic finite element analysis of axially vibrating nonlocal rods, Finite Elem. Anal. Des. 63 (1) (2013) 42–50.
[36] S. Pradhan, Nonlocal finite element analysis and small scale effects of CNTS with Timoshenko beam theory, Finite Elem. Anal. Des. 50 (2012) 8–20.
[37] R. Ansari, R. Rajabiehfard, B. Arash, Nonlocal finite element model for vibrations of embedded multi-layered graphene sheets, Comput. Mater. Sci. 49 (4) (2010) 831–838.
[38] L. Meirovitch, Principles and Techniques of Vibrations, Prentice-Hall International, Inc., New Jersey, 1997.
[39] M. Géradin, D. Rixen, Mechanical Vibrations, 2nd Edition, John Wiley & Sons, New York, NY, 1997 (Translation of: Théorie des Vibrations).
[40] M. Petyt, Introduction to Finite Element Vibration Analysis, Cambridge University Press, Cambridge, UK, 1998.
[41] J.N. Reddy, Nonlocal theories for bending, buckling and vibration of beams, Int. J. Eng. Sci. 45 (2–8) (2007) 288–307.
[42] S. Narendar, S. Gopalakrishnan, Non local scale effects on ultrasonic wave characteristics nanorods, Phys. E: Low-Dimens. Syst. Nanostruct. 42 (5) (2010) 1601–1604.
[43] D. Dawe, Matrix and Finite Element Displacement Analysis of Structures, Oxford University Press, Oxford, UK, 1984.
[44] P. Karaoglu, M. Aydogdu, On the forced vibration of carbon nanotubes via a non-local euler-bernoulli beam model, Proc. Inst. Mech. Eng. Part C—J. Mech. Eng. Sci. 224 (C2) (2010) 497–503.
[45] L. Rayleigh, Theory of Sound (Two Volumes), 1945th Edition, Dover Publications, New York, 1877.
[46] S. Adhikari, Structural Dynamic Analysis with Generalized Damping Models: Analysis, Wiley ISTE, UK, 2013 (368 pages) ⟨http://eu.wiley.com/WileyCDA/WileyTitle/productCd-1848215215.html⟩.
[47] O.C. Zienkiewicz, R.L. Taylor, The Finite Element Method, 4th Edition, McGraw-Hill, London, 1991.
[48] T.K. Caughey, M.E.J. O'Kelly, Classical normal modes in damped linear dynamic systems, Trans. ASME, J. Appl. Mech. 32 (1965) 583–588.
[49] S. Adhikari, Damping modelling using generalized proportional damping, J. Sound Vib. 293 (1–2) (2006) 156–170.
[50] R. Chowdhury, S. Adhikari, F. Scarpa, Vibrational analysis of Zno nanotubes: a molecular mechanics approach, Appl. Phys. A 102 (2) (2011) 301–308.
[51] R. Chowdhury, S. Adhikari, C.Y. Wang, F. Scarpa, A molecular mechanics approach for the vibration of single walled carbon nanotubes, Comput. Mater. Sci. 48 (4) (2010) 730–735.
[52] T. Murmu, S. Adhikari, M. McCarthy, Vibration response of double-walled carbon nanotubes subjected to an externally applied longitudinal magnetic field: a nonlocal elasticity approach, J. Sound Vib. 331 (23) (2012) 5069–5086.
[53] R. Chowdhury, S. Adhikari, F. Scarpa, M.I. Friswell, Transverse vibration of single layer graphene sheets, J. Phys. D: Appl. Phys. 44 (20) (2011). 205401: 1-11.
[54] K. Kiani, Small-scale effect on the vibration of thin nanoplates subjected to a moving nanoparticle via nonlocal continuum theory, J. Sound Vib. 330 (20) (2011) 4896–4914.